

# A general estimator for the right endpoint – with an application to supercentenarian women’s records

Isabel Fraga Alves, CEAUL, DEIO, FCUL, University of Lisbon, [isabel.alves@fc.ul.pt](mailto:isabel.alves@fc.ul.pt)

Cláudia Neves, University of Reading, UK

## Abstract

We extend the right endpoint estimator introduced in Fraga Alves and Neves (Statist. Sinica 24:1811–1835, 2014) to a suitable endpoint estimator for any light-tailed distribution function belonging to some domain of attraction induced by the extreme value theorem. This stretch enables a general estimator of the finite right endpoint, which does not require estimation of the (supposedly non-positive) extreme value index. The asymptotic properties of this endpoint estimator are derived and its finite sample performance evaluated by means of simulations. The latter conveys that the adopted endpoint estimator works remarkably well in case the true extreme value index stays above  $-1/2$ , embracing the most common cases in practical applications. An illustration is provided through a brief extreme value analysis of supercentenarian women data.

**KEY WORDS AND PHRASES:** Extreme value theory Semi-parametric estimation Tail estimation Regular variation Monte Carlo simulation Human lifespan

## 1 Introduction

The extreme value theorem with contributions from [Fisher and Tippett, 1928, Gnedenko, 1943, de Haan, 1970], and its counterpart for exceedances above a threshold [Balkema and de Haan, 1974], ascertain that inference about rare events can be delivered by the highest (or lowest) observations in the sample. While restricting attention to the large rare events, the theoretical framework provided by the extreme value theorem reads as follows. If a non-degenerate limit is achieved for the maximum  $X_{n,n}$  of a sample of  $n$  independent and identically distributed random variables  $(X_1, X_2, \dots, X_n)$ , provided a suitable location-scale normalization, then the limiting distribution must be one of the following: Gumbel, Fréchet or (negative) Weibull. In other words, if there exist constants  $a_n > 0$ ,  $b_n \in \mathbb{R}$  such that  $\lim_{n \rightarrow \infty} F^n(a_n x + b_n) = G(x)$ , for all  $x$ ,  $G$  non-degenerate, then  $G$  is one of the only possible three distribution functions:

$$\begin{aligned} \Lambda(x) &= \exp\{-\exp(-x)\}, & x \in \mathbb{R}, \\ \Phi_\alpha(x) &= \exp\{-x^{-\alpha}\}, & x > 0, \quad \alpha > 0, \\ \Psi_\alpha(x) &= \exp\{-(-x)^\alpha\}, & x < 0, \quad \alpha > 0. \end{aligned} \tag{1}$$

Redefining the constants  $a_n > 0$  and  $b_n \in \mathbb{R}$ , then the above Weibull, Fréchet and Gumbel distribution functions, respectively, can be nested in a one-parameter family of distributions, the

Generalized Extreme Value (GEV) distribution with distribution function  $G_\gamma(x) := \exp\{-(1 + \gamma x)^{-1/\gamma}\}$ ,  $1 + \gamma x > 0$ ,  $\gamma \in \mathbb{R}$ . We then say that  $F$  is in the (max-)domain of attraction of  $G_\gamma$ , for some  $\gamma \in \mathbb{R}$  (notation:  $F \in \mathcal{D}(G_\gamma)$ ). Observe that for  $\gamma < 0$ ,  $\gamma = 0$  and  $\gamma > 0$ , the GEV distribution function reduces again to Weibull, Gumbel and Fréchet distribution functions, respectively. Hence, the GEV distribution is a unifying model that encompasses the only three possible types of extreme value distributions. If  $F \in \mathcal{D}(G_\gamma)$  with  $\gamma > 0$ , then the distribution function  $F$  is heavy-tailed, i.e.,  $F$  has a power-law decaying tail with infinite right endpoint. On the opposite end,  $\gamma < 0$  refers to short tails which must detain a finite right endpoint. Uniform and Beta distributions are examples of distributions belonging to the Weibull domain of attraction. The Gumbel domain of attraction encloses a great variety of distributions, ranging from light-tailed distributions such as the Normal distribution, the exponential distribution, to moderately heavy distributions such as the Lognormal (see p. 145 in [Embrechts et al., 1997]). Following a semi-parametric approach, the only assumption made is that  $F \in \mathcal{D}(G_\gamma)$  for some  $\gamma \in \mathbb{R}$ . The theory of regular variation [Bingham et al., 1987, de Haan, 1970, de Haan and Ferreira, 2006], provides necessary and sufficient conditions for  $F \in \mathcal{D}(G_\gamma)$ . Let  $U$  be the tail quantile function, defined by the (generalized) inverse of  $1/(1-F)$ ,

$$U(t) := \left( \frac{1}{1-F} \right)^{\leftarrow} (t) = F^{\leftarrow} \left( 1 - \frac{1}{t} \right), \quad \text{for } t > 1.$$

Then,  $F \in \mathcal{D}(G_\gamma)$  if and only if there exists a positive measurable function  $a(\cdot)$  such that the condition of *extended regular variation*

$$\lim_{t \rightarrow \infty} \frac{U(tx) - U(t)}{a(t)} = \frac{x^\gamma - 1}{\gamma}, \quad (2)$$

holds for all  $x > 0$  (notation:  $U \in ERV_\gamma$ ). From the above limiting relation, where the right hand-side coincides with the  $U$ -function of the Generalized Pareto distribution (GPD), we clearly see that the focus of our statistics of extremes is on the largest observations: given a sufficiently high threshold, the excesses above this threshold behave approximately as observations from GPD, which enables us to discard the remainder lower part of the sample. We shall base our statistical inference exclusively on a tiny top portion of the original sample, in the sense that we shall keep the number  $k$  of sufficiently large observations, thus preserving the top sample fraction  $k/n$ , where  $n$  (assumed a large number) denotes the original sample size. However, retaining only the number  $k$  of upper observations means that we further need an increasing  $k$  for the purpose of applying the large number probabilistic theory. Therefore, for estimating the right endpoint  $x^F$ , we shall assume that  $k$  is an *intermediate* sequence of positive integers  $k = k_n$  such that  $k \rightarrow \infty$  and  $k/n \rightarrow 0$ , as  $n \rightarrow \infty$ . The right endpoint of a distribution function  $F$  is defined as

$$x^F := \sup\{x : F(x) < 1\},$$

which, in terms of high quantiles, is given by  $x^F = \lim_{t \rightarrow \infty} U(t) = U(\infty)$ , with  $x^F \leq \infty$ . This paper deals with semi-parametric approach to the estimation of the finite right endpoint  $x^F$  of a distribution  $F \in \mathcal{D}(G_\gamma)_{\gamma \leq 0}$ . Although the general endpoint estimator  $\hat{x}^F$  is not asymptotically normal for all values of  $\gamma < 0$ , it nonetheless proves to be a useful tool in terms of applications. One possibility would be the case study by [Einmahl and Magnus, 2008] aiming at the estimation of the ultimate records in several events in Athletics. A more obvious estimator for

the right endpoint is the sample maximum. In fact, [de Haan and Ferreira, 2006] point out in their Remark 4.5.5 that using the sample maximum  $X_{n,n}$  to estimate  $x^F$  in case  $\gamma < -1/2$  is approximately equivalent to using the moment related estimator for the endpoint. The striking feature of the proposed general estimator is that it avoids the nuisance of changing “tail estimation-goggles” each time we are dealing with yet another sample, possibly generated by a distribution in a different domain of attraction. The case study by [Einmahl and Magnus, 2008] could well benefit from using the same endpoint estimator at all instances, in all events, free of any liability about the estimated extreme value index  $\gamma$ . An application of the general estimator to the long jump ultimate record has been provided by [Fraga Alves et al., 2013].

The outline of the paper is as follows. Section 2 introduces the general estimator  $\hat{x}^F$  and addresses a class of endpoint estimators  $\hat{x}^*$ , widely used under a semi-parametric framework. Large sample results for  $\hat{x}^F$  are presented in Section 3. Section 5 gives a brief illustration of the exact behaviour our general endpoint estimator, in the context of human lifespan, based on extreme value statistical analysis of *supercentenarian women data*. Finally, in Section 6, we list several concluding remarks. Appendix A encloses all the proofs of the large sample results in Section 3, Appendix B complements the main text and Appendix C emulates the supercentenarian women data via a simulated sample from a specific parametric model.

## 2 Endpoint estimation

Several estimators for the right endpoint  $x^F$  of a light-tailed distribution attached to an extreme value index  $\gamma < 0$  are available in the literature, e.g. [Hall, 1982, Cai et al., 2013, de Haan and Ferreira, 2006]. These estimators often bear on the extreme value condition (2) with  $x = x(t) \rightarrow \infty$ , as  $t \rightarrow \infty$ : since  $\gamma < 0$  entails that  $\lim_{t \rightarrow \infty} U(t) = U(\infty)$  exists finite, then relation (2) rephrases as

$$\lim_{t \rightarrow \infty} \frac{U(\infty) - U(t)}{a(t)} = -\frac{1}{\gamma}.$$

A valid estimator for the right endpoint  $x^F = U(\infty)$  thus arises by making  $t = n/k$  in the approximate equality below

$$U(\infty) \approx U(t) - \frac{a(t)}{\gamma}$$

and then replacing  $U(n/k)$ ,  $a(n/k)$  and  $\gamma$  with suitable estimators, i.e.

$$\hat{x}^* = \hat{U}\left(\frac{n}{k}\right) - \frac{\hat{a}\left(\frac{n}{k}\right)}{\hat{\gamma}} \quad (3)$$

(cf. Section 4.5 of [de Haan and Ferreira, 2006]).

There is however one estimator for the right endpoint  $x^F$  that does not depend on the estimation of the extreme value index  $\gamma$ . This estimator, introduced in [Fraga Alves and Neves, 2014], is primarily tailored for light-tailed distributions in the Gumbel domain of attraction. The study of consistency and asymptotic distribution of this same endpoint estimator is the main objective in this paper, while it aims at covering the whole scenario in extremes, thus providing a unified estimation procedure for the right endpoint in the widest possible case of  $\gamma \leq 0$ .

We now set forth some notation. Let  $F$  be the distribution function of the random variable  $X$ . Let  $X_{1,n} \leq X_{2,n} \leq \dots \leq X_{n,n}$  be the  $n$ -th ascending order statistics associated with the sample  $X_1, \dots, X_n$  of  $n$  independent and identically distributed copies of  $X$ . Hence the general

right endpoint estimator:

$$\hat{x}^F := X_{n,n} + X_{n-k,n} - \frac{1}{\log 2} \sum_{i=0}^{k-1} \log\left(1 + \frac{1}{k+i}\right) X_{n-k-i,n}. \quad (4)$$

Defining  $a_{i,k} := \log\left(\frac{k+i+1}{k+i}\right) / \log 2$ , the endpoint estimator  $\hat{x}^F$  in (4) can be expressed in the equivalent form

$$\hat{x}^F := X_{n,n} + \sum_{i=0}^{k-1} a_{i,k} (X_{n-k,n} - X_{n-k-i,n}) \quad \text{with} \quad \sum_{i=0}^{k-1} a_{i,k} = 1. \quad (5)$$

From the non-negativeness of the weighted spacings in the sum in (5), it is clear that estimator  $\hat{x}^F$  is greater than  $X_{n,n}$ , which constitutes a major advantage in the usual right endpoint estimation of a distribution belonging to the Weibull domain of attraction.

Therefore, the estimator  $\hat{x}^F$  defined in (4) can be seen as a real asset in the context of semi-parametric estimation of the finite right endpoint, embracing all distributions connected by a non-positive extreme value index  $\gamma$ , which gains by far a broader spectrum of application to the usual alternatives.

### 3 Results on the general endpoint estimator

This section contains a Proposition and the main Theorem of this paper, giving accounts of strong consistency and sometimes asymptotic normality (we will see that the limiting normal distribution is only attained for  $\gamma < -1/2$ ) of the general endpoint estimator defined in (4). All the proofs are postponed to Appendix A.

**Proposition 1.** *Suppose  $x^F = U(\infty) := \lim_{t \rightarrow \infty} U(t)$  exists finite. Assume that the extended regular variation property (2) holds with  $\gamma \leq 0$ . If  $k = k_n \rightarrow \infty$ ,  $k_n/n \rightarrow 0$ , as  $n \rightarrow \infty$  then the following almost sure convergence holds with respect to  $\hat{x}^F$  defined in (4):*

$$\hat{x}^F \xrightarrow[n \rightarrow \infty]{a.s.} x^F,$$

then  $\hat{x}^F$  is a consistent estimator for  $x^F < \infty$ , i.e.  $\hat{x}^F \xrightarrow[n \rightarrow \infty]{P} x^F$ .

We now require a second order refinement of condition (2) and auxiliary second order conditions in order to have a grasp at the speed of convergence in (2). In particular, we assume there exists a positive or negative function  $A_0$  with  $\lim_{t \rightarrow \infty} A_0(t) = 0$  such that for each  $x > 0$ ,

$$\lim_{t \rightarrow \infty} \frac{\frac{U(tx) - U(t)}{a_0(t)} - \frac{x^\gamma - 1}{\gamma}}{A_0(t)} = \Psi_{\gamma, \rho}^*(x), \quad (6)$$

where  $\rho$  is a non-positive parameter and with

$$\Psi_{\gamma, \rho}^*(x) := \begin{cases} \frac{x^{\gamma+\rho} - 1}{\gamma + \rho}, & \gamma + \rho \neq 0, \rho < 0, \\ \log x, & \gamma + \rho = 0, \rho < 0, \\ \frac{1}{\gamma} x^\gamma \log x, & \rho = 0 \neq \gamma, \\ \frac{1}{2} (\log x)^2, & \gamma = \rho = 0, \end{cases}$$

$$a_0(t) := \begin{cases} a(t)(1 - A_0(t)), & \rho < 0, \\ a(t)(1 - A_0(t)/\gamma), & \rho = 0 \neq \gamma, \\ a(t), & \gamma = \rho = 0. \end{cases}$$

Moreover,  $|A_0| \in RV_\rho$  and

$$\lim_{t \rightarrow \infty} \frac{\frac{a_0(tx)}{a_0(t)} - x^\gamma}{A_0(t)} = x^\gamma \frac{x^\rho - 1}{\rho}, \quad (7)$$

for all  $x > 0$  [cf. Theorem 2.3.3 and Corollary 2.3.5 of [de Haan and Ferreira, 2006]]. If (6) holds with  $\gamma < 0$  then, provided  $x = x(t) \rightarrow \infty$ ,

$$\lim_{t \rightarrow \infty} \frac{\frac{U(\infty) - U(t)}{a_0(t)} + \frac{1}{\gamma}}{A_0(t)} = \Psi_{\gamma, \rho}^*(\infty) := -\frac{1}{\gamma + \rho} I_{\{\rho < 0\}} \quad (8)$$

by similar arguments of Lemma 4.5.4 of [de Haan and Ferreira, 2006], with  $I_A$  denoting the indicator function which is equal to 1 if  $A$  holds true and is equal to zero otherwise.

**Theorem 2.** *Let  $F$  be a distribution function in the Weibull domain of attraction, i.e.,  $F \in \mathcal{D}(G_\gamma)$  with  $\gamma < 0$ . Suppose  $U$  satisfies condition (6) with  $\gamma < 0$  and, in this sequence, assume that (8) holds. We define*

$$h(\gamma) := \frac{1}{\gamma} \left( \frac{2^{-\gamma} - 1}{\gamma \log 2} + 1 \right). \quad (9)$$

If the intermediate sequence  $k = k_n$  is such that  $\sqrt{k_n} A_0(n/k_n) \rightarrow \lambda \in \mathbb{R}$ , then

$$k^{\min(-\gamma, 1/2)} \left( \frac{\hat{x}^F - x^F}{a_0\left(\frac{n}{k}\right)} - h(\gamma) \right) \xrightarrow[n \rightarrow \infty]{d} W I_{\{\gamma \geq -1/2\}} + (N - \lambda b_{\gamma, \rho}) I_{\{\gamma \leq -1/2\}},$$

where  $W$  is a max-stable Weibull random variable, with distribution function  $\exp\{-(\gamma x)^{-1/\gamma}\}$  for  $x < 0$ ,  $N$  is a normal random variable with zero mean and variance given by

$$\text{Var}(N) = 1 + \frac{2}{\gamma (\log 2)^2} \left( \frac{2^{-(2\gamma+1)} - 1}{2\gamma + 1} - \frac{2^{-(\gamma+1)} - 1}{\gamma + 1} + \frac{\log 2}{\sqrt{2}} (2^{-\gamma} - 1) \right). \quad (10)$$

and  $b_{\gamma, \rho}$  is defined as

$$b_{\gamma, \rho} := \frac{1}{\log 2} \int_{1/2}^1 \Psi_{\gamma, \rho}^*\left(\frac{1}{2s}\right) \frac{ds}{s} = \begin{cases} \frac{1}{\gamma + \rho} \left( \frac{1}{\log 2} \frac{1 - 2^{-(\gamma + \rho)}}{\gamma + \rho} - 1 \right), & \rho < 0, \\ \frac{1}{\gamma^3 \log 2} \left( 2^{-\gamma} (\log 2^\gamma + 1) - 1 \right), & \rho = 0. \end{cases}$$

Moreover, the random variables  $W$  and  $N$  are independent.

**Remark 3.** *The same normalization by  $(a_0(n/k))^{-1}$ , corresponding to  $\gamma = 0$ , has been obtained by [Fraga Alves and Neves, 2014] in order to attain a Gumbel limiting distribution.*

**Corollary 4.** *Under the conditions of Theorem 2,*

$$\frac{\sqrt{k} \left( \frac{\hat{x}^F - x^F}{a_0\left(\frac{n}{k}\right)} - h(\gamma) \right)}{k^{(\gamma+1/2)^+}} \xrightarrow[n \rightarrow \infty]{d} R,$$

where  $a^+ := \max(a, 0)$  and  $R$  denotes a random variable with the following characterization:

1. Case  $-1/2 < \gamma < 0$ : the random variable  $R$  is max-stable Weibull, with distribution function  $\exp\{-(\gamma x)^{-1/\gamma}\}$  for  $x < 0$ , with mean  $\Gamma(1-\gamma)/\gamma$  and variance equal to  $\gamma^{-2}(\Gamma(1-2\gamma) - \Gamma^2(1-\gamma))$ . Here and throughout,  $\Gamma(\cdot)$  denotes the upper incomplete gamma function evaluated at zero, i.e.  $\Gamma(a) = \int_0^\infty t^{a-1}e^{-t} dt$ ,  $a > 0$ .
2. Case  $\gamma < -1/2$ : the random variable  $R$  has normal distribution with mean  $-\lambda b_{\gamma,\rho}$  and variance given in (10).
3. Case  $\gamma = -1/2$ : the random variable  $R$  is the sum of the two cases above, taken as independent components, which yields a random part with mean  $\Gamma(1/2) - \lambda b_{-1/2,\rho} = \sqrt{\pi} - \lambda b_{-1/2,\rho}$  and variance equal to

$$5 - \pi + 4[1 + (1/\sqrt{2} - 1)(2 + \log 2)/\log 2]/\log 2.$$

**Remark 5.** The function  $h(\gamma)$  is monotone decreasing for all  $\gamma < 0$ . Taking into account the statement of Theorem 2, an adaptive reduced bias estimator based on the general estimator  $\hat{x}_F$  is given by  $\hat{x}_{RB1}^F = \hat{x}_F - h(\hat{\gamma})\hat{a}(n/k)$ . The dominant part comes from the scale function  $a(n/k)$  which, in case of  $\gamma = 0$ , determines very slow convergence. We have conducted several simulations in this respect. These indicate that this bias correction has a very limited effect, in what can be consider as a residual improvement. Later on, in Section 5.3, we will handle with a second order bias correction.

## 4 Comparative study via simulation

In this section we study the exact properties of the general endpoint estimator  $\hat{x}^F$  defined in (4). To this end, we are going to consider four models already worked out in [Girard et al., 2011, Girard et al., 2012]. In the latter, the simulation presented only cover the case of EVI equal to  $-1$ . At the present stage we are interested in studying the exact performance of the endpoint estimator for different ranges of negative EVI. A number of combinations between model and parameters are assigned in order to obtain two distinct values of the negative EVI, particularly  $\gamma = -1/2, -1/5$ . Another model with  $\gamma = -0.1$  is given in Appendix C in connection with our example of application. The case  $\gamma = 0$  has been extensively studied in [Fraga Alves and Neves, 2014]. Our key examples are displayed in the scheme below.

- **Model 1**, with distribution function  $F_1(x) = 1 - [1 + (-x)^{-\tau_1}]^{-\tau_2}$ ,  $x < 0$ ,  $\tau_1, \tau_2 > 0$ . The EVI is  $-1/(\tau_1\tau_2)$  and the endpoint  $x^{F_1} = 0$ .
- **Model 2**, with distribution function  $F_2(x) = 1 - \int_{-\infty}^{\log(1-1/x)} \lambda^2 t e^{-\lambda t} dt$ ,  $x < 0$ ,  $\lambda > 0$ . The EVI is  $-1/\lambda$  and the endpoint  $x^{F_2} = 0$ . Moreover,  $X \stackrel{d}{=} -1/(e^Z - 1)$ , where  $Z$  is Gamma(*shape* = 2, *rate* =  $\lambda$ ) distributed.
- **Model 3**, with distribution function  $F_3(x) = 1 - [1 + (\frac{1}{x} - 1)^{-\tau_1}]^{-\tau_2}$ ,  $x \in (0, 1)$ ,  $\tau_1, \tau_2 > 0$ . The EVI is  $-1/(\tau_1\tau_2)$  and the endpoint is  $x^{F_3} = 1$ .

- **Model 4**, with distribution function  $F_4(x) = 1 - \int_{-\infty}^{-\log(1-x)} \lambda^2 t e^{-\lambda t} dt$ ,  $x \in (0, 1)$ ,  $\lambda > 0$ . The EVI is  $-1/\lambda$  and the endpoint is  $x^{F_4} = 1$ . A random variable  $X$  has distribution function  $F_4$  if  $X \stackrel{d}{=} 1 - e^{-Z}$ , with  $Z$  a Gamma(*shape* = 2, *rate* =  $\lambda$ ) random variable.

At a first glance, the four models considered above may indicate that only a modest simulation study was undertaken but these were in fact taken as key examples from an exhaustive set of simulations.

The finite sample performance of the general estimator (notation: FAN) will be compared with the naive maximum estimator  $X_{n,n}$  (notation: MAX) and the estimator  $\hat{x}^*$  (notation: MOM) introduced in [Dekkers et al., 1989] (see Theorem 5.2 and expression (4.8)):

$$\hat{x}^* := X_{n-k,n} - \frac{X_{n-k,n} M_{n,k}^{(1)} (1 - \hat{\gamma}_{n,k}^M)}{\hat{\gamma}_{n,k}^M}. \quad (11)$$

This estimator  $\hat{x}^*$  evolves from (3) by replacing  $\hat{\gamma}$  and  $\hat{a}(n/k)$  with the moment related estimators for  $\gamma \in \mathbb{R}$  and  $a(n/k)$ , notably the moment estimator for the EVI:

$$\hat{\gamma}_{n,k}^M := M_{n,k}^{(1)} + 1 - \frac{1}{2} \left\{ 1 - \frac{(M_{n,k}^{(1)})^2}{M_{n,k}^{(2)}} \right\}^{-1},$$

where

$$M_{n,k}^{(r)} := \frac{1}{k} \sum_{i=0}^{k-1} \left\{ \log(X_{n-i,n}/X_{n-k,n}) \right\}^r, \quad r = 1, 2. \quad (12)$$

[see Section 4.5 of [de Haan and Ferreira, 2006] and references therein].

The MOM estimator  $\hat{x}^*$  for the finite right endpoint has already been applied to a lifespan study by [Aarssen and de Haan, 1994]. Their Proposition A.2 (b), expression (A.8) and Lemma A.3 deemed the MOM endpoint estimator as most adequate for values of the EVI between  $-1/2$  and 0. Furthermore, the MOM and MAX estimators were also considered in [Girard et al., 2011, Girard et al., 2012]. On the contrary to what happens with the endpoint estimators proposed in [Girard et al., 2011, Girard et al., 2012], the three estimators, MAX, FAN and MOM, are all based on a certain number  $k^*$  of top order statistics (o.s.), and do not require the knowledge of the entire sample. This is usually the case in practice as in many applications the only observations available are the ones for the largest events. One example in this respect arises from the analysis of records in sports [see e.g. [Einmahl and Magnus, 2008]], in which a very small amount of top observations is known. In this sequence, the naive estimator MAX depends only on the first top extremal o.s. ( $k^* = 1$ ), whereas the MOM and FAN endpoint estimators are functions of the  $k^* = k + 1$  and  $k^* = 2k$  intermediate o.s., respectively.

Inspired in the numeric examples in [Girard et al., 2011, Girard et al., 2012], we have generated  $N = 500$  replications of a random sample with size  $n = 1000$ , from the designated models 1 up to 4. Then the average  $L^1$ -error, given by

$$E(k^*) := \frac{1}{N} \sum_{j=1}^N |\varepsilon(j, k^*)|, \quad \text{where} \quad \varepsilon(j, k^*) := \hat{x}_{k^*}(j) - x^F, \quad k^* \leq n,$$

Table 1: Average  $L^1$ -errors

Model	MAX	FAN	MOM
Model 1 ( $x^F = 0$ )			
$(\tau_1, \tau_2) = (2, 1)$	0.030	0.014	0.026
$(\tau_1, \tau_2) = (5, 1)$	0.227	0.042	0.050
Model 2 ( $x^F = 0$ )			
$\lambda = 2$	0.009	0.005	0.008
$\lambda = 5$	0.171	0.041	0.110
Model 3 ( $x^F = 1$ )			
$(\tau_1, \tau_2) = (2, 1)$	0.028	0.011	0.040
$(\tau_1, \tau_2) = (5, 1)$	0.189	0.131	0.144
Model 4 ( $x^F = 1$ )			
$\lambda = 2$	0.009	0.005	0.014
$\lambda = 5$	0.144	0.047	0.135

was obtained. Each  $x_{k^*}(j)$  denotes the endpoint estimator evaluated at the  $j$ -th replicate, for all values of  $k^*$ . We have also computed “optimal” values of  $k^*$  as the minimizer of the average  $L^1$ -error, i.e.  $k_0^* := \operatorname{argmin}\{E(k^*), k^* \leq n\}$ . Once the estimator MAX entails  $k^* = 1$ , the optimality criterium does not play a role. Models (eight selected models) and results are all displayed in Table 1. The FAN general estimator seems to yield better results than MAX or MOM estimators. The comparison of the exact behavior of the adopted endpoint estimators (at the “optimal” threshold  $k_0^*$  for MOM and FAN) is depicted in the boxplots of the associated errors  $\varepsilon(j, k_0^*)$ ,  $j = 1, \dots, N$ . These graphical tools, displayed in Figures 1 and 2 lead to the conclusion that the MAX estimator always underestimates the true value of the right endpoint  $x^F$ , as expected. MOM and FAN estimators present distinct performances at the optimal levels  $k_0^*$ . At optimal levels  $k_0^*$ , FAN estimates are not so spread out as the MOM ones, the latter revealing large variability.

Figures 3 and 4 display the *average  $L^1$ -error* as functions of the number  $k^*$  of upper o.s. used in the estimation, while corresponding mean squared errors (MSE) are depicted in Figures 5-6. From these results, it is clear that the MOM endpoint estimator presents large variability in upper part of the sample, contrasting with the small variance of the proposed FAN estimator. The four models addressed here correspond to  $\operatorname{EVI} = -1/2, -1/5$ . On the other hand, both MOM and FAN estimators show increasing  $L^1$ -error with increasing of  $k^*$ , a common feature in extreme semi-parametric estimators. Again, the more general endpoint estimator FAN tends to return values with quite low average  $L^1$ -error and MSE, in connection with  $\operatorname{EVI} = -1/2, -1/5$ . In fact, Figures 3 – 6 not only provide us with a snapshot for this specific choice of  $\operatorname{EVI}$  values, but also allow to foresee the estimates behaviour for the  $\operatorname{EVI}$ s in between, once we screen the plots from the top to the bottom in each Figure. The boxplots in Figures 1 and 2 already suggested this possibility: the outliers marked in these boxplots seems to move from lower to

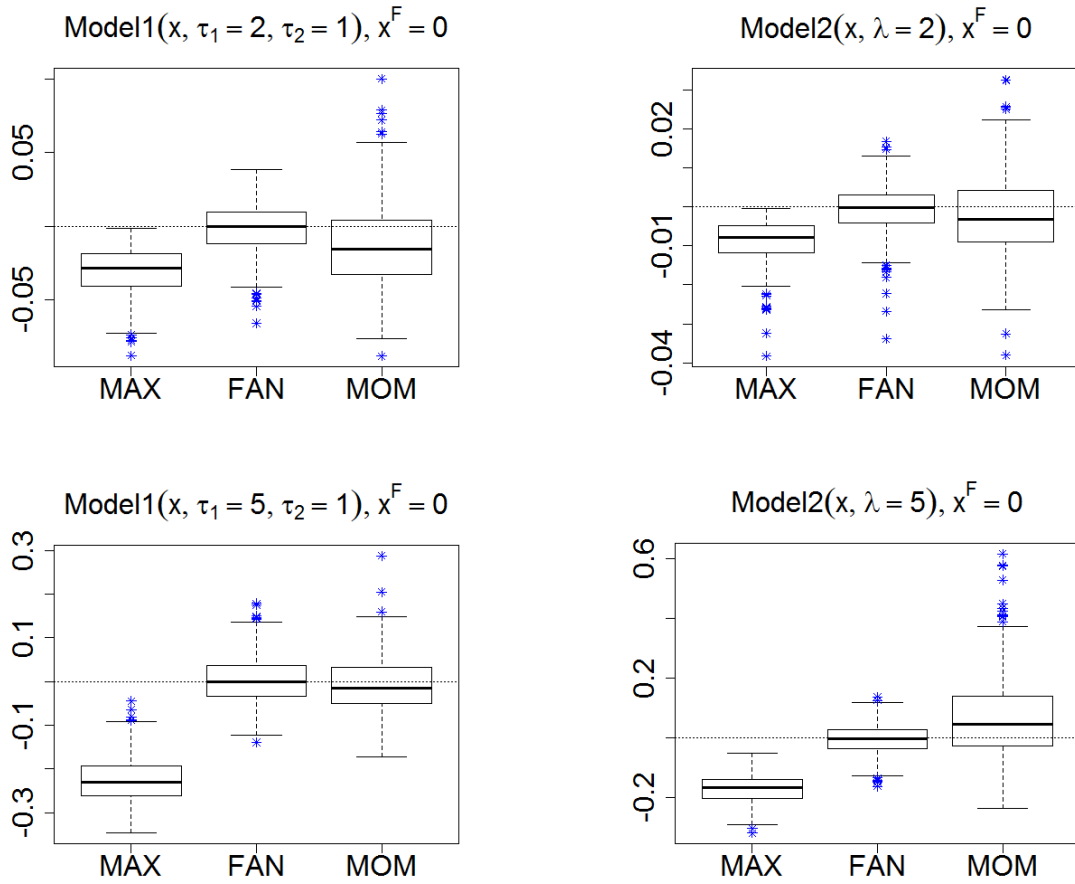


Figure 1: Model 1 (*left*) and Model 2 (*right*)  $x^{F_1} = x^{F_2} = x^F = 0$ : Boxplots of  $\varepsilon(j, k_0^*)$ ,  $j = 1, \dots, N$ , for MAX, MOM and FAN estimates.

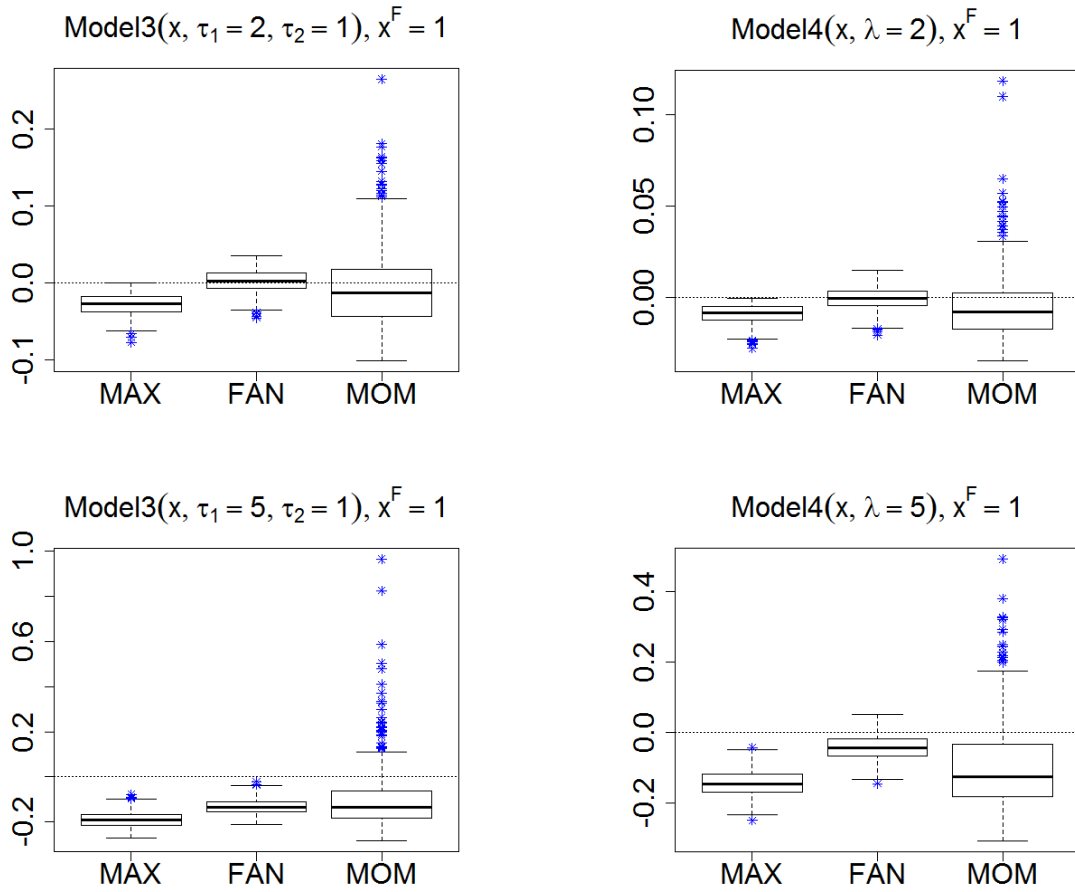


Figure 2: Model 3 (*left*) and Model 4 (*right*);  $x^{F_3} = x^{F_4} = x^F = 1$ : Boxplots of  $\varepsilon(j, k_0^*)$ ,  $j = 1, \dots, N$ , for MAX, MOM and FAN estimates.

larger values of optimal bias  $\varepsilon(\cdot, k_0^*)$  as we progress on increasing EVI.

Altogether, for all the distributions considered in the Weibull max-domain of attraction, the general endpoint estimator FAN tends to surpass the reminder two estimators, both in terms of absolute bias and variability. This is particularly true for a EVI close to zero, as it would be expected from the one estimator primarily tailored to tackle the endpoint estimation problem in the Gumbel domain [Fraga Alves and Neves, 2014]. Furthermore, the FAN estimator seems to work remarkably well under a fairly negative EVI, considering that this is a general estimator which does not accommodate any specific information about the true value  $\gamma = \text{EVI}$ . The overall performance of the MOM endpoint estimator is clearly damaged by its large variance.

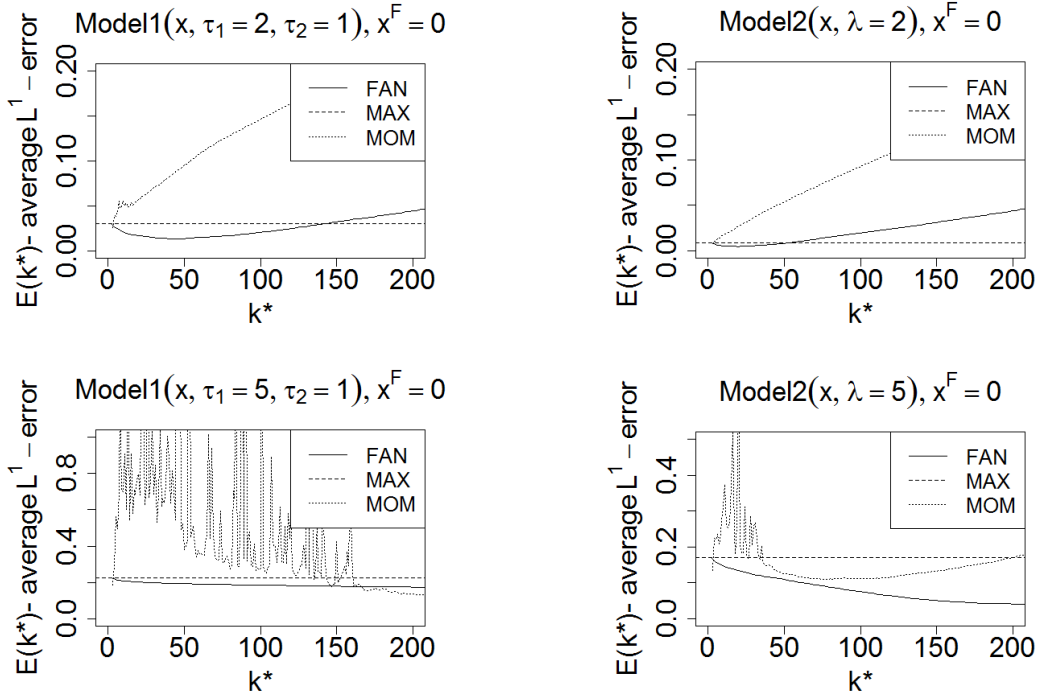


Figure 3: Model 1 (*left*) and Model 2 (*right*);  $x^{F_1} = x^{F_2} = x^F = 0$ :  $E(k^*)$  plotted against  $k^* \leq n/5$ .

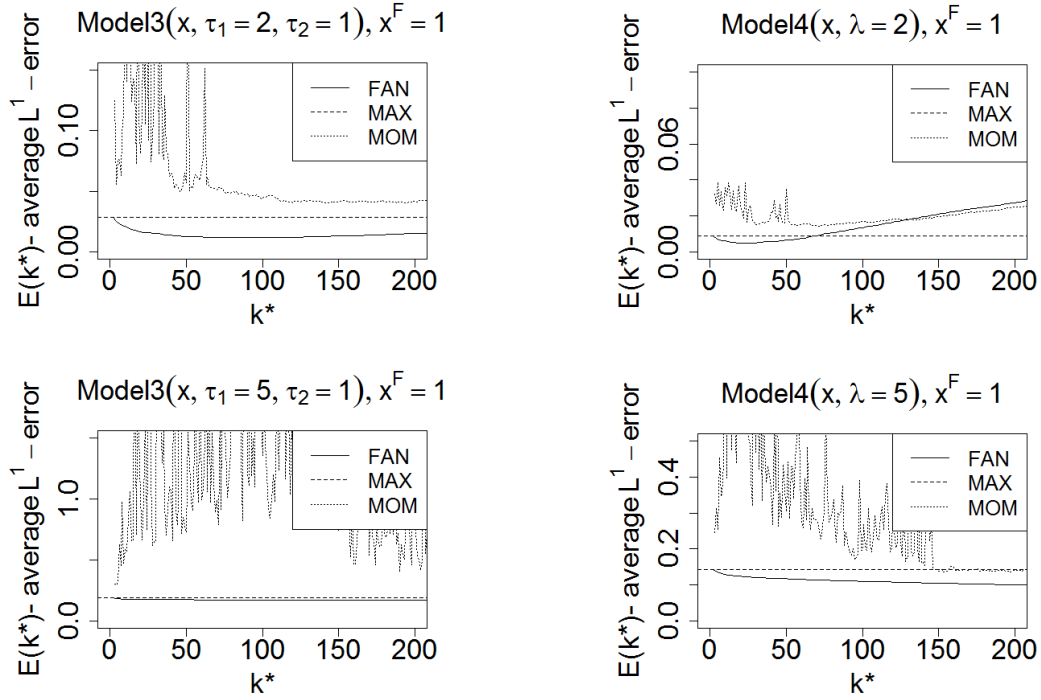


Figure 4: Model 3 (left) and Model 4 (right);  $x^{F_3} = x^{F_4} = x^F = 1$ :  $E(k^*)$  plotted against  $k^* \leq n/5$ .

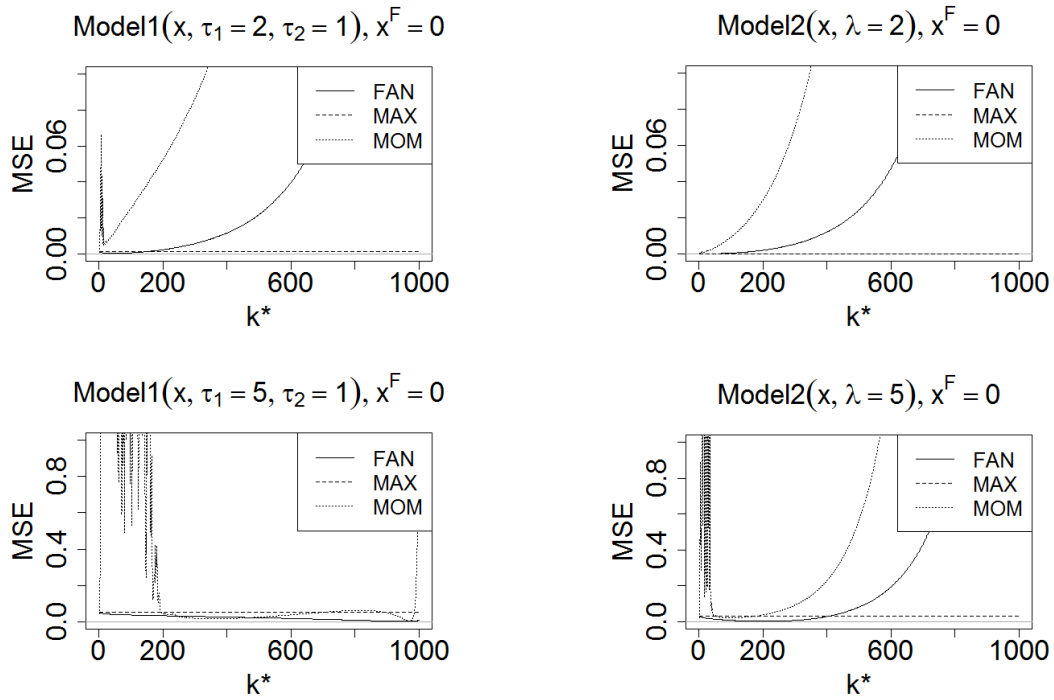


Figure 5: Models 1 (left) and 2 (right): mean squared error (MSE) as function of the upper o.s.  $k^*$ ,  $k^* \leq n$ .

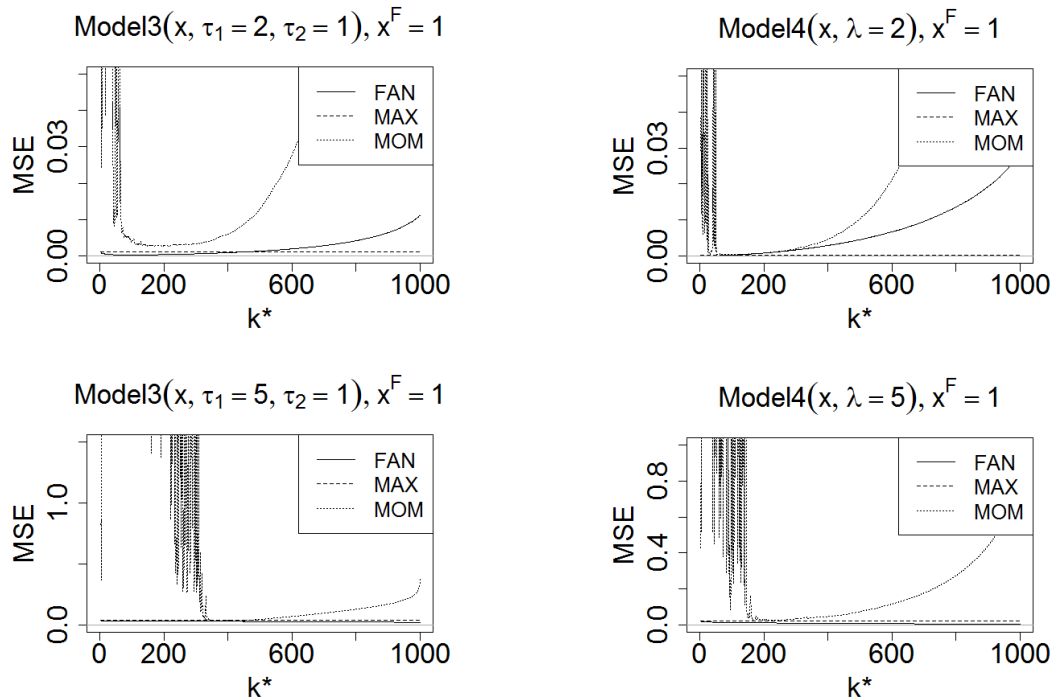


Figure 6: Models 3 (*left*) and 4 (*right*): mean squared error (MSE) as function of the upper o.s.  $k^*$ ,  $k^* \leq n$ .

The possibility of returning non-admissible values, i.e., values below the observed sample maximum may also account for the poor performance of the MOM in this study. Once  $\hat{x}^*$  depends directly on the estimated EVI, one could think that the most plausible reason for this misfunction should be a possible associated positive  $\hat{\gamma} \equiv \hat{\gamma}_{n,k}^M$ . Although this in fact accounts for the reported issue, it does not fully explain  $\hat{x}^* < x_{n,n}$ , for a wide range of thresholds or  $k$  values. Taking for key examples the models 3 and 4, it is noted that for a broadband of thresholds, an estimate of the endpoint value below the maximum is not at all associated with a positive estimated EVI. The complementary simulation study addressing the frequency of occurrences of the type  $\hat{x}^* < x_{n,n}$ , in parallel with  $\hat{\gamma}_{n,k}^M > 0$ , it is presented in Appendix B (see Figures B.1 and B.2). To overcome this issue in applications, the value of  $\hat{x}^*$  is thus replaced by the sample maximum  $x_{n,n}$ , in which case there is no effective contribution from the MOM estimator. This particularly occurs with underlying models in the Weibull domain of attraction with almost null EVI.

## 5 Case study: supercentenarian women lifespan

This section is devoted to the illustration of our methodology using lifespan times. It is not our purpose to make expert statements or issue binding judgement about human lifespan times.

The terms “life expectancy” and “lifespan” describe two entirely different concepts, although people tend to use these terms interchangeably. Life expectancy refers to the number of years a person is expected to live, based on the statistical average. Lifespan, on the other hand, refers to the maximum number of years that a person can potentially expect to live based on the greatest number of years anyone has lived. Formally, in the gerontology literature, maximum lifespan

potential (MLSP) represents an operational definition for the verified age of the longest lived individual for a species ([Olshansky et al., 1990b]) and, in this sense, acts as a theoretical upper limit to life time. The oldest documented age reached by any living individual is 122 years, meaning humans are said to have a maximal lifespan (MLSP) of 122 years. Several authors have stated that in spite of the increasing “life expectancy”, the “maximum human lifespan” has not much changed. According to [Troen and Cristafalo, 2001] some biodemographic estimates predict that elimination of most of the major diseases such as cancer, cardiovascular disease, and diabetes would add no more than 10 years to the average life expectancy, but would not affect MLSP ([Olshansky et al., 1990a], [Troen and Cristafalo, 2001]). Other researchers go further enough to hypothesize that mortality will be compressed against that fixed upper limit to life time ([Fries, 1980]). [Wilmoth and Robine, 2003] defend a possible world trend in maximum lifespan, although their claim basis is a Swedish long series of data; moreover, the authors keep open if the Swedish trend is a typical one for the whole world, or the world records are higher than the Swedish ones merely because they are drawn from larger population.

Above all, there is still plenty of scope to assess significance of other covariates, like the negative impact of obesity and epidemic diseases on the rise in life expectancy trends and the possible impact on the MLSP. What researchers seems to agree on is the need for better data, since at present, there is insufficient data available on the extreme elderly population. We should keep in mind that age is often misreported and at the time the current centenerians (and *supercentenarians*) were born, record keeping was less complete than it is nowadays. A procedure for detecting and estimating a trend in extremes, using a semiparametric approach, and thus very compatible with our setting has been recently introduced by [de Haan et al., 2015]. This method for assessing the presence of a trend in extremes is proposed along side with an application to daily rainfall. However, in order to be able to apply it and say something more about a possible trend in the supercentenarian women’s records, we would need much more observations than those available in the database, in order to meet the minimal requirements of this method.

Therefore, in our illustration we do not intend to make conclusions for a specific cohort of individuals in time or space or any other type of serial studies. We will focus on illustrating and investigating what are sensible bounds for MLSP, the upper limit of the human life time distribution, given the current state of the art. Bearing on the extreme value statistical analysis of *supercentenarians*, we would give tentative answers to impeding questions of this sort:

*Does this distribution have a finite right endpoint? In case the latter holds true, how can we estimate it? What might be a reasonable upper bound for the actual right endpoint of human lifespan, given the our accumulated knowledge until present day?*

At this point, some assumptions are needed on the right tail of the lifetime distribution, which is the focus of extreme value theory. EVT statistical procedures lead us, not only to a point estimate, but also and more important to confidence intervals stemming from asymptotic arguments. The latter require a large sample size. Our data regards the oldest of the old human survivors, the so-called *supercentenarians*, defined as persons aged 110 or older. In the adventure of human life, women are largely distanced from men: supercentenarians are mostly women; they represent around 90% of supercentenarians, as of January 1, 2014, in Table B - Verified Supercentenarians by Gerontology Research Group (GRG) (<http://www.grg.org/Adams/Tables.htm>).

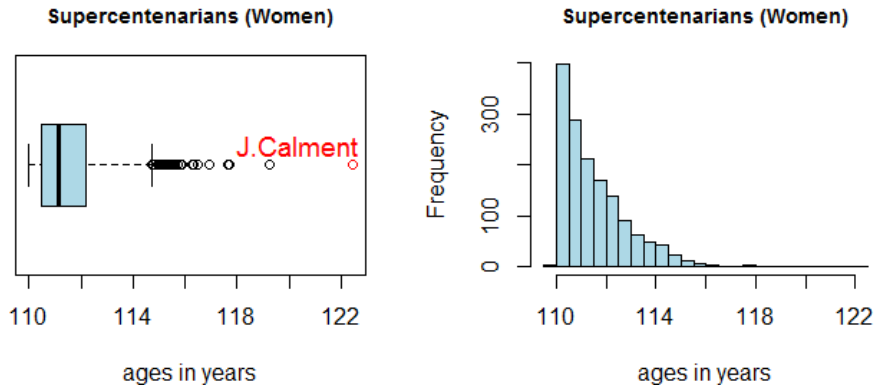


Figure 7: Boxplot (*left*) and Histogram (*right*): verified supercentenarians, as of January 1, 2014.

Stephen Coles, a specialist in tracking human supercentenarians and co-founder of the Supercentenarian Research Foundation (SRF), referred to the supercentenarians as “the most extreme example of human longevity that we know about, the oldest old”. In [Coles, 2011], the value 122 is referred to as the “Calment Limit” for human longevity (what is designated here as the MLSP), which is supported by the fact that nobody has come even close that extreme age over the last 17 years. It is also mentioned that, by his research experience “supercentenarians had virtually nothing in common: they had different occupations, lifestyles, religions and so on, regardless the common factor of long-lived relatives.” Also, according to [Vaupel, 2011] “The explosion in very long life has already begun”, although by his perspective “we cannot see much beyond 122.” With our modest contribution we expect to unveil how much time can be *potentially* ahead of us, giving some upper limit to the endpoint of human life distribution. Our data set of oldest people comprises  $n = 1497$  records, the age in days of *verified supercentenarians (women)*, as of January 1, 2014, in Table B by GRG, merged with Table E of Recent Deaths, as of September 21, 2014.

## 5.1 Testing finiteness in the right endpoint

In Biology, theories of ageing are mainly divided into two groups: damage theories and program theories. According to damage theories, we age because our systems break down over time; so, if damage theories are true, we can survive any longer by avoiding damaging our organism. Program theories consider that we age because there is an inbuilt mechanism that tells us to die; according to that, we cannot survive longer than the upper limit of longevity despite our best efforts (see [Hanayama, 2013]). [Kaufmann and Reiss, 2007] also discussed the issue of whether the right endpoint of the life span is infinite, for which they analyzed mortality data from West Germany. The estimated shape parameter within the Generalized Pareto model is equal to  $-0.08$  and the right endpoint of the estimated beta distribution is equal to 122 years, an estimate that fits well to the worldwide reported life span of the most famous record-holder, the Frenchwoman Jeanne-Louise Calment (122 years and 164 days) who was born in Arles on Feb. 21, 1875 and died in Arles on Aug. 4, 1997. However, [Kaufmann and Reiss, 2007] did not conclude categorically that human lifespan has a finite upper limit, arguing that by using the concept of penultimate distributions we can show that an infinite upper limit is well compatible with extreme value theory. They carry on, however, pointing out a Beta distribution. [Aarssen and de Haan, 1994] analyzed lifespan data from the Netherlands using

statistical methods under the extreme value theory umbrella. [Aarssen and de Haan, 1994] showed that there is a finite age limit, tackled with reasonable confidence bounds in the 113–124 year span, a conclusion confined to the years of birth 1877 – 1881 in the Netherlands.

Our first aim is to assess about the finiteness of the right endpoint of the distribution function  $F$  underlying the women lifespan data. In the detection of a possibly finite upper bound for our data, we will proceed via a semiparametric approach, meaning that we essentially assume that  $F$  belongs to some max-domain of attraction. According to this setup, it is only natural to expect that such a tentative answer will depend on how deep we are willing to go into the original sample of supercentenarian women’s records. This question can be reformulated as follows. How may we selected the top sample fraction to use in our testing and estimation methods? One grounding result in this respect is that all the estimators we are adopting, are all consistent under the assumption that  $k = k_n$  is an intermediate sequence of positive integers, i.e.  $k = k_n$  is such that  $k_n \rightarrow \infty$  and  $k_n/n \rightarrow 0$ , as  $n \rightarrow \infty$ . The testing procedures we wish to apply also bear on this rather usual assumption in statistics of extremes.

In a first stage, we shall address the statistical choice of max-domains of attraction. There are many proposals in the literature for testing procedures aiming at the selection of a suitable domain of attraction. For a global view on this topic, we refer the overviews about extreme values testing available in [Husler and Peng, 2008] and [Neves and Fraga Alves, 2008]. A possible estimation of the EVI  $\gamma$  returning negative values, could give a first insight of the tail feature for  $F$ . However, we recall that EVI estimation is not a requirement for the general endpoint estimation prescribed in (4). Thus, for the time being, we will follow testing procedures which do not appeal for a direct EVI estimation. In the present illustrative example, we use the testing procedures of the hypothesis

$$H_0 : F \in \mathcal{D}_M(G_0) \quad vs \quad H_1 : F \in \mathcal{D}_M(G_\gamma)_{\gamma \neq 0} .$$

by [Neves et al., 2006] and [Neves and Fraga Alves, 2007]).

The moments of the excesses over the random threshold  $X_{n-k,n}$  are defined as  $M_j := \frac{1}{k} \sum_{i=1}^k (X_{n-i+1,n} - X_{n-k,n})^j$ ,  $j = 1, 2$ . These constitute the building blocks of the three test statistics we are going to use. Namely, Greenwood(G), Hasofer&Wang(HW) and Ratio(R), which are defined as follows:

$$G := \frac{M_2}{(M_1)^2} \quad HW := \frac{1}{k(G-1)} \quad R := \frac{X_{n,n} - X_{n-k,n}}{M_1} .$$

Under  $H_0$ , the standardized versions of Greenwood and Hasofer&Wang statistics are asymptotically standard normal  $G^* := \sqrt{k/4}(G-2) \xrightarrow[n \rightarrow \infty]{d} Z_1 \sim N(0, 1)$   $HW^* := \sqrt{k/4}(k HW - 1) \xrightarrow[n \rightarrow \infty]{d} Z_2 \sim N(0, 1)$ , whereas the normalized version of the latter ratio is asymptotically Gumbel, i.e.  $R^* := R - \log k \xrightarrow[n \rightarrow \infty]{d} Z_3 \sim \Lambda(z) = \exp(-\exp(-z)), z \in \mathbb{R}$ . Moreover,  $HW^*$  returns values to the right direction for distributions in Weibull domain, whereas  $G^*$  and  $R^*$  go towards left for short tailed distributions in the Weibull domain. Formally, approximately  $\alpha$ -significant tests can be conducted through the rejection regions  $|G^*| \geq z_{1-\alpha/2}$ ,  $|HW^*| \geq z_{1-\alpha/2}$ , for normal critical values  $z_\epsilon := \Phi^{-1}(\epsilon)$ , and  $R^* \leq \omega_{\alpha/2} \vee R^* \geq \omega_{1-\alpha/2}$ , with Gumbel quantiles  $\omega_\epsilon := \Lambda^{-1}(\epsilon)$ . Figure 8 depicts the sample paths of the statistics,  $G^*$ ,  $HW^*$  and  $R^*$ , as well as their  $\alpha = 1\%$  critical values. We can conclude that there is enough evidence to reject the Gumbel domain of attraction hypothesis in favour of a bounded short-tail in Weibull domain. This follows from

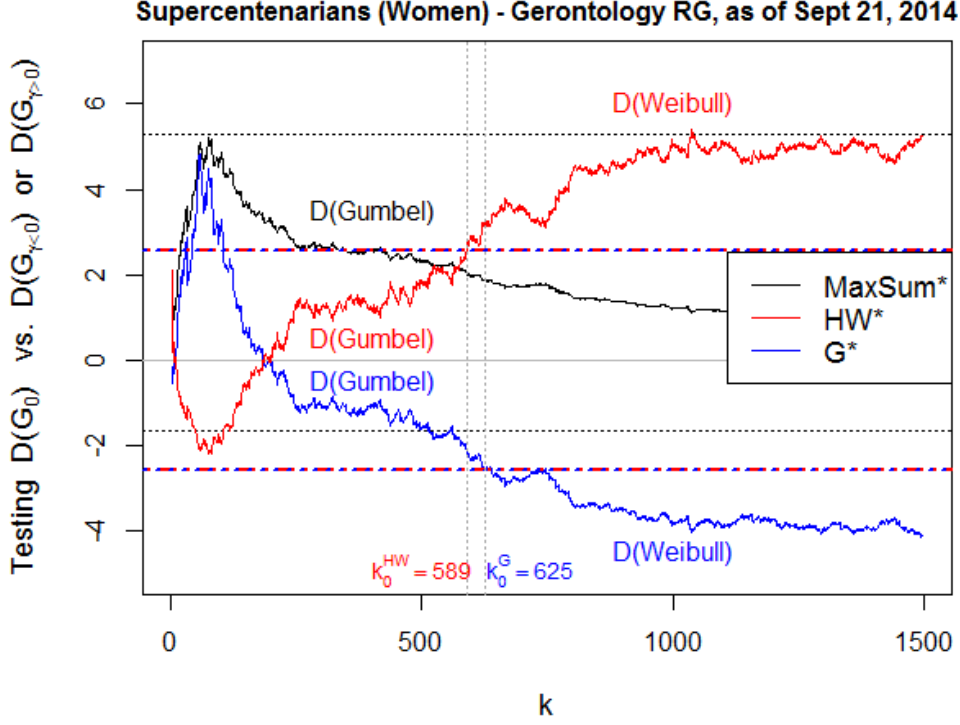


Figure 8: Testing max-domains of attraction, for verified supercentenarians data set.

G and HW tests essentially, at the suitable intermediate values of  $k_0^G = 625$  and  $k_0^{HW} = 589$ , respectively. The suitable choice of  $k$  comes from the approach by [Wang, 1995], where  $k$  is deemed to be selected at the value  $k_0$  from which on the null hypothesis is rejected. Concerning the third statistic,  $R^*$ , the conclusion is more conservative, conducting to a non rejection of the null hypothesis, meaning that the right endpoint could be finite or not, in a context of the Gumbel domain.

The following testing approach was introduced in [Neves and Pereira, 2010], precisely for detecting finiteness of the right endpoint for tails in Weibull or Gumbel domains. More formally, the testing problem

$$H_0 : F \in \mathcal{D}_M(G_0), x^F = \infty \quad vs \quad H_1 : F \in \mathcal{D}_M(G_\gamma)_{\gamma \leq 0}, x^F < \infty .$$

is tackled using two test statistics which rely on the first two log-moments  $M^{(r)} \equiv M_{n,k}^{(r)}$ ,  $r = 1, 2$ , previously defined in (12). Hence, the tests  $T_1$  and  $T_2$  are given in terms of

$$T_1 := \frac{1}{k} \sum_{i=1}^k \frac{X_{n-i,n} - X_{n-k,n} - T}{X_{n,n} - X_{n-k,n}}, \quad \text{with } T := X_{n-k,n} \frac{M^{(1)}}{2} \left( 1 - \frac{[M^{(1)}]^2}{M^{(2)}} \right)^{-1} .$$

and

$$T_2 := \frac{1}{k} \sum_{i=1}^{k-1} i \frac{X_{n-i+1,n} - X_{n-i,n}}{X_{n-k,n}} .$$

Under  $H_0$ , the standardized versions are asymptotically normal, i.e.,  $T_1^* := \sqrt{k} \log k T_1 \xrightarrow[n \rightarrow \infty]{d} N(0, 1)$

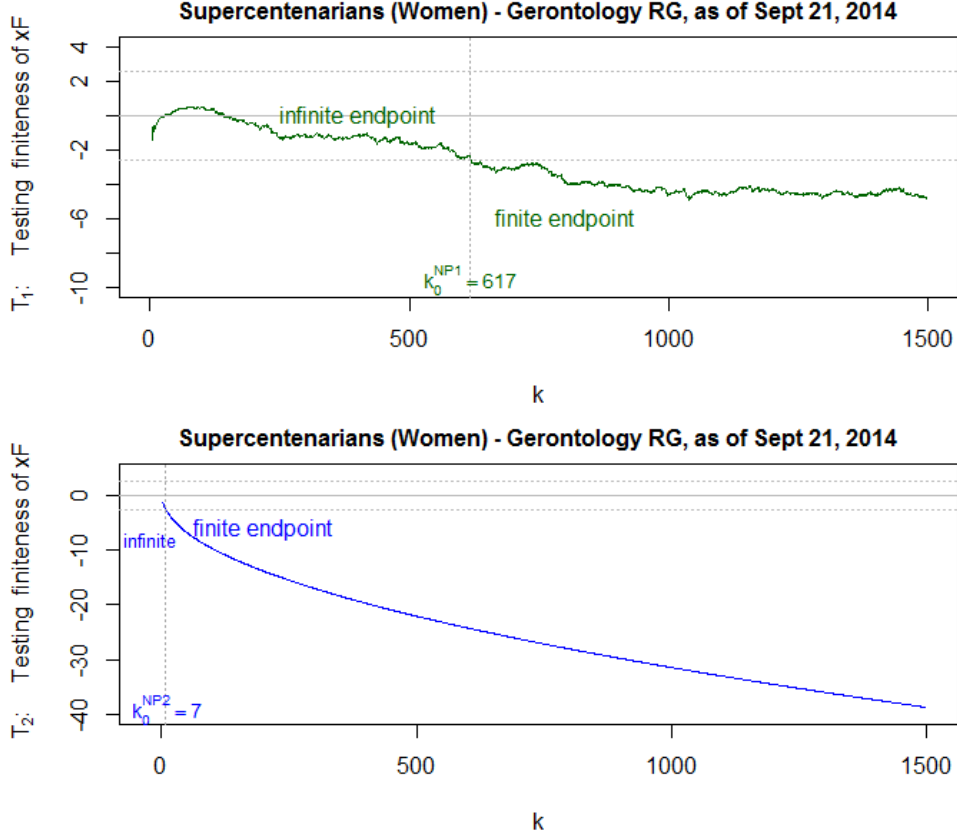


Figure 9: Detecting finiteness of right endpoint for verified supercentenarians data set.

and  $T_2^* := \sqrt{k} (\log(n/k) T_2 - 1) \xrightarrow[n \rightarrow \infty]{d} N(0, 1)$ . Moreover, both  $T_1^*$  and  $T_2^*$  inflect to the left for bounded tails in Weibull domain and to the right for Gumbel domain. In what follows, approximately  $\alpha$ -significant tests can be conducted through the rejection regions  $|T_j^*| \geq z_{1-\alpha/2}$ ,  $j = 1, 2$ .

In Figure 9 are depicted the sample paths of the 2 statistics,  $T_1^*$ ,  $T_2^*$ , and the  $\alpha = 1\%$  critical values, leading to rejection of infinite right endpoints in Gumbel Domain, in favour of bounded short-tails in Weibull domain, supported by convenient intermediate values on, respectively  $k_0^{NP1} = 617$  and  $k_0^{NP2} = 7$ , the former being more conservative. The choice of a convenient single  $k_{opt}$  for a subsequent endpoint inference approach will be on the smallest  $k$  at which the previous analysis yields a finite right endpoint, simultaneously for all the adopted testing methods; i.e., the maximum of the previous referred values,  $k_{opt} := \max\{k_0^G, k_0^{HW}, k_0^{NP1}, k_0^{NP2}\} = 625$ . Based not only on testing procedures, but also on EVI estimation that have been done in complement, it is reasonable to conclude that lifespan distribution belongs to Weibull domain of attraction and thus possesses a finite right endpoint  $x^F$ , based on the top 625 values of our data set. Now we will try to answer

*What is the maximum human lifespan? That is, how long can humans live, given today's state of the art or given the present cumulative knowledge from this phenomena?*

Note that here it is not supposed to do here a chronological study for temporal prediction. After the previous testing steps and choice of the threshold  $k_{opt} = 625$ , we will present similar graphics for endpoint estimation, illustrating the flat and smooth behaviour of  $\hat{x}^F$  defined in

(4), always returning values above the naive endpoint estimator, the “Calment limit” of 122.4 years.

## 5.2 Endpoint estimation of women’s records

Figure 10 displays the graphic of the comparative exact behaviour of  $\hat{x}^F$  (notation: `xF_FAN`) for the supercentenarians data set. We underline that it is not supposed to give full insight about the available endpoint estimators. Such an exhaustive comparative study goes out the scope of the present illustrative example. Nevertheless, we find sensible to provide information yielded by other semiparametric estimators, which may serve as a good complement. Namely, we consider as before the moment endpoint estimator (notation: `xF_MOM`) defined in (11).

From Figure 10 it is clear the flat pattern of `xF_FAN` estimator not influenced by a beforehand EVI estimation, contrasting with the volatile feature of `xF_MOM`. It is also marked the point estimate  $\hat{x}_{\text{FAN}}^F = 122.9$  years built on the 625  $k$ -largest observations and the “Calment limit”, always below the sample path of  $\hat{x}_{\text{FAN}}^F$ , a feature not shared by `xF_MOM` which returns a large amount of inadmissible values, i.e., below the sample maximum; concerning the exact behaviour of `xF_MOM` it should be mentioned that this is a pattern present also in the simulations, with a significative proportion of returned inadmissible values, even that the EVI estimation gives back negative values and consequently a foreseen finite endpoint; this issue is sometimes surpassed by taking  $\tilde{x}^* := \max(\hat{x}^*, x_{n,n})$ , which may be not more informative than the available sample maximum; this is the case in the present application, with two range of  $k$  values below the “Calment limit”: a top region that expands around the 200 upper values, which is not surprising, since it was found that EVI estimated by  $\gamma_{n,k}^M$ , for instance, is positive, but also a large non-informative region of almost half of the sample around  $k = 625$  on, although in this range the  $\gamma$  estimates exhibit a flat pattern clearly negative around  $-0.1$ ,  $-0.2$ . This global picture for EVI estimation through  $\gamma_{n,k}^M$  is included in Appendix C, Figure C.3.

## 5.3 Reduced bias estimation and confidence bandwidth for *lifespan*

Based on the asymptotic results of Theorem 4, for  $-1/2 < \gamma < 0$ , we draw approximated confidence bandwidths for  $x^F$ . In fact, although  $\hat{x}^F$  estimator does not depend itself on external estimation of the EVI, the asymptotic distribution of our endpoint estimator is strongly dependent on  $\gamma$ . Next to this, we will consider a new adaptive second order reduced bias estimator based on the general  $\hat{x}_F$  and motivated by the results of Theorem 4, for  $-1/2 < \gamma < 0$ . Remark that in the case of negative  $\gamma$  values close to zero, an usual situation in most practical applications, the convergence of the normalized general estimator  $\hat{x}_F$  may be very slow, since it is headed both by the function  $a \in RV_\gamma$  and a power for the intermediate sequence  $k^\gamma$ . Adding to this, it should be mentioned that the limit r.v.  $W$ , with Weibull distribution, possesses a non null expected value, given by  $\Gamma(1 - \gamma)/\gamma$ , with  $\hat{x}^F$  admitting the asymptotic representation

$$\hat{x}^F = x^F + h(\gamma)a_0\left(\frac{n}{k}\right) + a_0\left(\frac{n}{k}\right)k^\gamma W + o_p\left(a_0\left(\frac{n}{k}\right)k^\gamma\right),$$

with  $h(\gamma)$  defined in (9). Thus, suggested by this representation, a new adaptive second order reduced bias estimator based on the general  $\hat{x}_F$  is:

$$\hat{x}_{RB2}^F = \hat{x}^F - h(\hat{\gamma})\hat{a}_0\left(\frac{n}{k}\right) - \frac{\Gamma(1-\hat{\gamma})}{\hat{\gamma}}\hat{a}_0\left(\frac{n}{k}\right)k^{\hat{\gamma}}.$$

## Supercentenarians (Women) - Gerontology RG, as of Sept 21, 2014

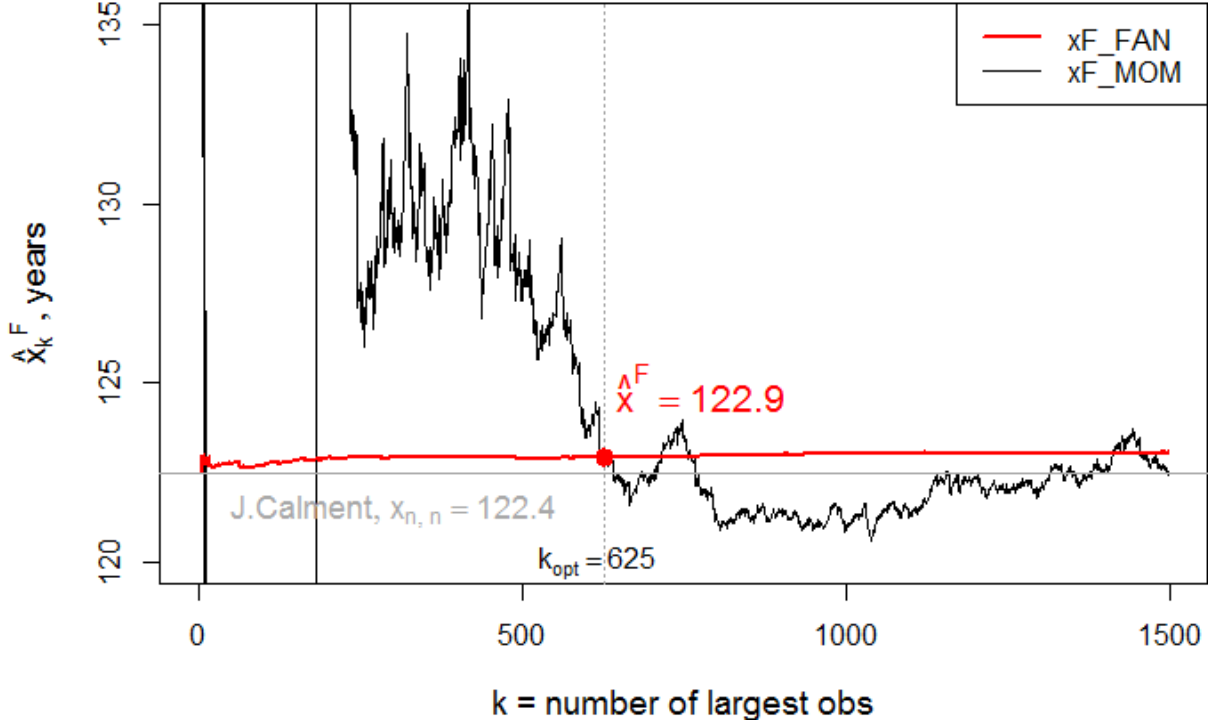


Figure 10: Endpoint estimation for verified supercentenarians data set.

Moreover, in this case an approximated  $(1 - \alpha)$ -confidence two-sided interval for  $x^F$  is given by

$$(CI_{inf}, CI_{sup}) = \left( \hat{x}^F - \hat{a}_0\left(\frac{n}{k}\right) [h(\hat{\gamma}) + k^{\hat{\gamma}} q_{1-\alpha/2}], \hat{x}^F - \hat{a}_0\left(\frac{n}{k}\right) [h(\hat{\gamma}) + k^{\hat{\gamma}} q_{\alpha/2}] \right),$$

with  $q_\varepsilon := (-\log \varepsilon)^{-\hat{\gamma}}/\hat{\gamma}$  replacing the  $\varepsilon$ -quantile of the Weibull limit distribution  $\exp[-(\gamma x)^{-1/\gamma}]$ ,  $\hat{a}_0(n/k) = X_{n-k,n} M_{n,k}^{(1)}(1 - \hat{\gamma}_{n,k}^M)$  and  $\hat{\gamma} = \gamma_{n,k}^M$ .

Figure 11 displays the sample path of  $\hat{x}_{RB2}^F$ , accompanied by the confidence bandwidth built on the confidence intervals for every  $k$ . In the graphic it is also marked the estimation for  $k_{opt} = 625$ , for which  $\gamma_{n,625}^M = -0.133$ ,  $(CI_{inf}, CI_{sup}) := (123.6, 128.8)$ .

We also mimicked the obtained results using one 1500 sized simulated sample from Model 3 ( $\tau_1 = 1, \tau_2 = 10$ ) presented in Section 4, with location 110 and a scale 20, from which was possible to compare the estimated results with the true values, and in particular with the  $x^F = 130$ . The simulated analysis is available in the Appendix C, Figures C.1-C.6 and Table 2.

### 5.4 An upper limit to *lifespan*

From the previous data analysis we would say that an upper value for the human lifespan should be no larger than 128.8 years. This gives some input beyond the achieved so far by Mrs. Calment of 122.4 years, and not surpassed for 17 years already. Adding to this, it should also be mentioned that the probability of exceeding the ‘‘Calment limit’’, even for a supercentenarian women, it is extremely low. This could also be supported by tail probability estimation using

## Supercentenarians (Women) - Gerontology RG, as of Sept 21, 2014

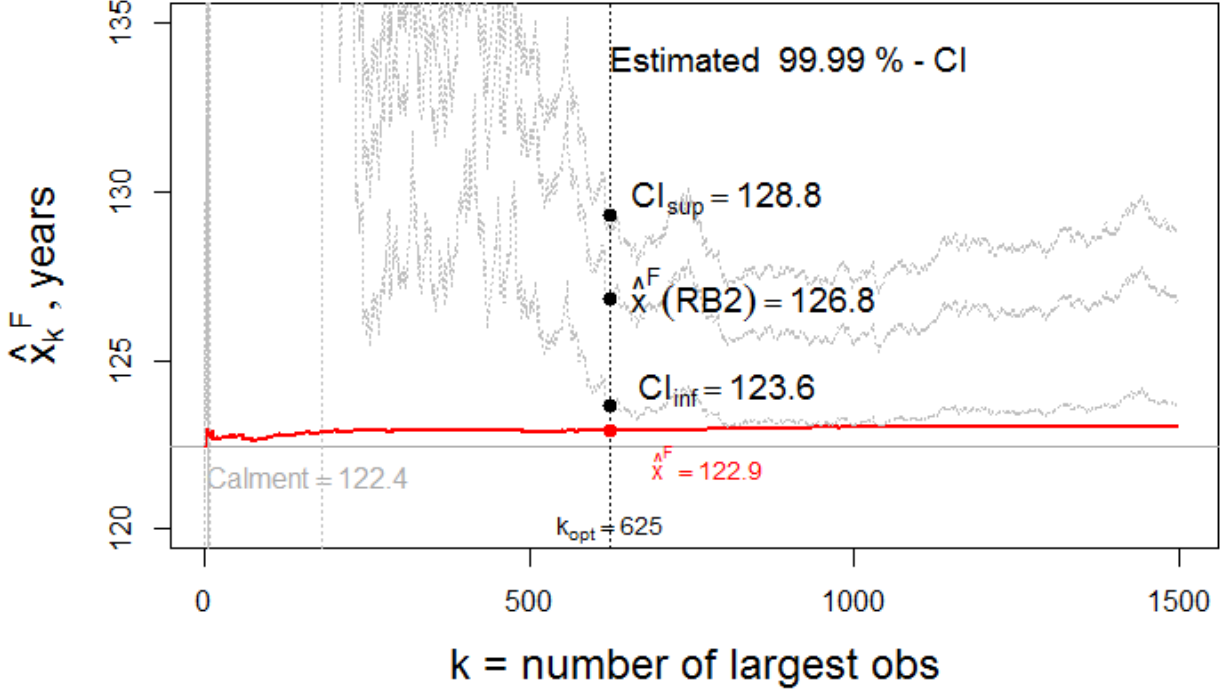


Figure 11: Endpoint Confidence Bandwidth for verified supercentenarians data set, with  $\gamma_{n,k}^M$ .

the semi-parametric estimator (see (4.4.1) in [de Haan and Ferreira, 2006] for details)

$$\hat{P}(X_s > 122.4)_n := \frac{k}{n} \left\{ \max \left( 0, 1 + \hat{\gamma}_{n,k}^M \frac{122.4 - X_{n-k,n}}{X_{n-k,n} M_{n,k}^{(1)} (1 - \hat{\gamma}_{n,k}^M)} \right) \right\}, \quad (13)$$

where  $X_s$  denotes time life for a supercentenarian women. In Figure 12 we depict the diagram of these probability estimates, for a wide range of largest age values of the 1497 verified supercentenarians data set, chosen to make possible to distinguish the chart trace from straight zero line.

## 6 Concluding remarks

We have extended the scope of application for the estimator of right endpoint  $x^F$  from [Fraga Alves and Neves, 2014], therein specially designed for Gumbel domain, in order to embrace the case of the Weibull domain. The study of consistency and asymptotic distribution of the general endpoint estimator  $\hat{x}^F$  defined in (4) now renders a unified estimation procedure for the right endpoint in the general scenario of  $\gamma \leq 0$ . Our main findings are listed below.

- the general endpoint estimator does not require the estimation of the extreme value index. To the best of our knowledge, this is not the case with similar semi-parametric procedures available in the literature;

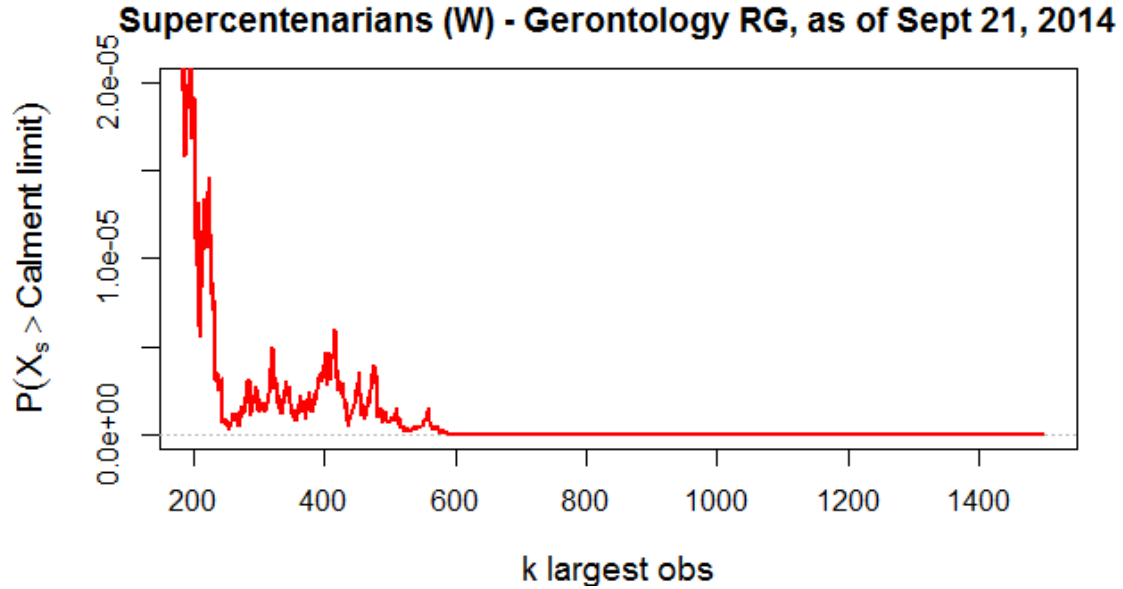


Figure 12: Probability of exceeding the “Calment limit”, for a supercentenarian women, given today’s state of the art.

- by construction, the estimator  $\hat{x}^F$  returns values bigger than the sample maximum  $X_{n,n}$ , a property seen as of great advantage to the most common common semi-parametric methodologies for right endpoint in Weibull max-domain;
- the simulation study reveals a good finite sample performance for the general endpoint estimator, ascertaining competitiveness both in terms of absolute bias and mean squared error;
- related to the previous, the general endpoint estimator performs better for distributions with  $\gamma > -1/2$ , which encompasses the most common cases in practice;
- given the usual flat pattern of the diagrams for the general endpoint estimator  $\hat{x}^F$  against the number  $k$  of top observations, the problem of choosing the most adequate  $k$  no longer plays a role;
- the application to lifespan data, together with the simulated sample from Model 3, illustrates how one can establish reasonable confidence bandwidths, built on the asymptotic results.

## Acknowledgements

Isabel Fraga Alves’ research is partially supported by national funds through the Fundação Nacional para a Ciência e Tecnologia, Portugal–FCT under the project PEst-OE/MAT/UI0006/2014.

## A Proofs of asymptotic results

This section is entirely dedicated to the proofs of the results introduced in Section 3. In what follows we find more convenient to consider the estimator  $\hat{x}^F$  in the functional form

$$\hat{x}^F = X_{n-k,n} - \frac{1}{\log 2} \int_0^1 (X_{n-[2ks],n} - X_{n-[ks],n}) \frac{ds}{s}, \quad (\text{A1})$$

where  $[a]$  denotes the integer part of  $a \in \mathbb{R}$  [more details about the representation (A1) can be obtained in [Fraga Alves and Neves, 2014]].

We note that if  $s \in [0, 1/(2k)[$ , then the integral in (A1) is equal to zero. Bearing this in mind, we write

$$\hat{x}^F = X_{n-k,n} - \frac{1}{\log 2} \int_{\frac{1}{2k}}^1 (X_{n-[2ks],n} - X_{n-[ks],n}) \frac{ds}{s}.$$

Moreover, if  $s \in [1/(2k), 1/k[$  then  $[ks] = 0$  (not depending on  $s$ ) and thus  $X_{n-[ks],n} = X_{n,n}$ . Therefore, we have that

$$\hat{x}^F = X_{n-k,n} - \frac{1}{\log 2} \left\{ \int_{\frac{1}{2k}}^{\frac{1}{k}} X_{n-[2ks],n} \frac{ds}{s} - X_{n,n} \int_{\frac{1}{2k}}^{\frac{1}{k}} \frac{ds}{s} + \int_{\frac{1}{k}}^1 (X_{n-[2ks],n} - X_{n-[ks],n}) \frac{ds}{s} \right\}. \quad (\text{A2})$$

With a suitable variable transform on the last integral, we can reassemble (A2) in a tidy manner:

$$\hat{x}^F = X_{n,n} + X_{n-k,n} - \frac{1}{\log 2} \int_{\frac{1}{2}}^1 X_{n-[2ks],n} \frac{ds}{s}. \quad (\text{A3})$$

This is the main algebraic expression that will be used to derive the asymptotic distribution of  $\hat{x}^F$  in the proof of Theorem 2, which is a natural consequence of the three random contributions in (A3).

**Proof of Proposition 1:** We see that the integral in the functional form (A3) satisfies the inequalities

$$(\log 2) X_{n-k,n} \leq \int_{\frac{1}{2}}^1 X_{n-[2ks],n} \frac{ds}{s} \leq (\log 2) X_{n-2k,n}.$$

Therefore, we obtain the following upper and lower bounds involving  $\hat{x}^F - x^F$ ,

$$X_{n,n} - x^F \leq \hat{x}^F - x^F \leq (X_{n,n} - x^F) + X_{n-k,n} - X_{n-2k,n},$$

and the result thus follows easily because the three order statistics  $X_{n,n}$ ,  $X_{n-k,n}$  and  $X_{n-2k,n}$  all converge almost surely to  $x^F$ , provided the intermediate nature of  $k = k_n$ .  $\square$

**Remark A.1.** *Alternative proof based on the functional form (5) of the  $k^* := 2k$  top order statistics: for the estimator defined in (5), strong consistence is assured by lower and upper*

bounds: on the one hand,

$$\begin{aligned}\hat{x}^F - x^F &= (X_{n,n} - x^F) + \left( X_{n-k,n} - \frac{1}{\log 2} \sum_{i=0}^{k-1} \log\left(\frac{k+i+1}{k+i}\right) X_{n-k-i,n} \right) \\ &\geq (X_{n,n} - x^F) + \left( X_{n-k,n} - X_{n-k,n} \frac{1}{\log 2} \sum_{i=0}^{k-1} \log\left(\frac{k+i+1}{k+i}\right) \right) = X_{n,n} - x^F\end{aligned}$$

and on the other hand,

$$\begin{aligned}\hat{x}^F - x^F &\leq (X_{n,n} - x^F) + \left( X_{n-k,n} - X_{n-2k+1,n} \frac{1}{\log 2} \sum_{i=0}^{k-1} \log\left(\frac{k+i+1}{k+i}\right) \right) \\ &= (X_{n,n} - x^F) + (X_{n-k,n} - X_{n-2k+1,n}) ;\end{aligned}$$

since for any intermediate  $k = k_n$  the order statistics  $X_{n,n}, X_{n-k,n}, X_{n-2k,n}$  converge almost surely to  $x^F$ , the result follows.

Before getting under way to the proof of the main theorem, we need to lay down some ground results. These comprise a Proposition and a Lemma regarding the case  $\gamma < 0$ , along with a further development of the condition of regular variation introduced in Section 3.

**Proposition A.2.** *Suppose  $X_{n,n}$  is the maximum of a random sample whose parent distribution function  $F$  detains finite right endpoint of  $F$ , i.e.  $x^F = U(\infty) < \infty$ . Assume the second order condition (6) holds with  $\gamma < 0$ . If  $k = k_n$  is such that, as  $n \rightarrow \infty$ ,  $k \rightarrow \infty$ ,  $k/n \rightarrow 0$  and  $\sqrt{k} A_0(n/k) \rightarrow \lambda \in \mathbb{R}$ , then*

1. for  $\gamma \geq -1/2$ , for each  $\varepsilon > 0$ ,

$$k^{-\gamma-\varepsilon} \left| \frac{X_{n,n} - x^F}{a_0\left(\frac{n}{k}\right)} \right| \xrightarrow[n \rightarrow \infty]{p} 0. \quad (\text{A4})$$

Moreover,

$$k^{-\gamma} \frac{X_{n,n} - x^F}{a_0\left(\frac{n}{k}\right)} \xrightarrow[n \rightarrow \infty]{d} \frac{Z^\gamma}{\gamma},$$

where  $Z$  denotes a standard Fréchet with distribution function  $\Phi_1$  as in (1).

2. for  $\gamma < -1/2$ ,

$$\sqrt{k} \left| \frac{X_{n,n} - x^F}{a_0\left(\frac{n}{k}\right)} \right| \xrightarrow[n \rightarrow \infty]{p} 0.$$

**Proof:** Owing to the well-known equality in distribution that  $X_{i,n} \stackrel{d}{=} U(Y_{i,n})$ ,  $i = 1, 2, \dots, n$ , with  $\{Y_{i,n}\}_{i=1}^n$  the  $n$ -th order statistics from a sample of  $n$  independent random variables with common (standard) Pareto distribution function given by  $1 - x^{-1}$ ,  $x \geq 1$ , then the following equality in distribution holds:

$$\frac{X_{n,n} - x^F}{a_0\left(\frac{n}{k}\right)} \stackrel{d}{=} \left\{ \frac{U\left(\frac{k}{n} Y_{n,n} \frac{n}{k}\right) - U\left(\frac{n}{k}\right)}{a_0\left(\frac{n}{k}\right)} + \frac{1}{\gamma} \right\} - \left\{ \frac{U(\infty) - U\left(\frac{n}{k}\right)}{a_0\left(\frac{n}{k}\right)} + \frac{1}{\gamma} \right\}.$$

Now we use conditions (6) and (8) with  $t$  replaced by  $n/k$  everywhere:

$$\begin{aligned} \frac{X_{n,n} - x^F}{a_0\left(\frac{n}{k}\right)} &\stackrel{d}{=} \left\{ \frac{k^\gamma (n^{-1}Y_{n,n})^\gamma - 1}{\gamma} + \frac{1}{\gamma} + A_0\left(\frac{n}{k}\right) \Psi_{\gamma,\rho}^* \left(\frac{k}{n} Y_{n,n}\right) (1 + o_p(1)) \right\} \\ &\quad - \left\{ A_0\left(\frac{n}{k}\right) \Psi_{\gamma,\rho}^*(\infty) (1 + o(1)) \right\} \\ &= \frac{k^\gamma (n^{-1}Y_{n,n})^\gamma}{\gamma} + A_0\left(\frac{n}{k}\right) \left\{ \Psi_{\gamma,\rho}^* \left(\frac{k}{n} Y_{n,n}\right) + \frac{1}{\gamma + \rho} I_{\{\rho < 0\}} \right\} + o_p\left(A_0\left(\frac{n}{k}\right)\right) \end{aligned}$$

We note at this stage that  $n^{-1}Y_{n,n}$  is asymptotically a Fréchet random variable with distribution function given by  $\Phi_1$  in (1). This non-degenerate limit yields  $(k/n)Y_{n,n}$  going to infinity with probability one, which implies in turn that  $\Psi_{\gamma,\rho}^* \left(k(n^{-1}Y_{n,n})\right) \rightarrow -(\gamma + \rho)^{-1} I_{\{\rho < 0\}}$ , as  $n \rightarrow \infty$ . Therefore, we obtain for  $\gamma \geq -1/2$ ,

$$k^{-\gamma} \frac{X_{n,n} - x^F}{a_0\left(\frac{n}{k}\right)} \stackrel{d}{=} \frac{(n^{-1}Y_{n,n})^\gamma}{\gamma} + o_p(k^{-\gamma-1/2}), \quad (\text{A5})$$

by virtue of  $\sqrt{k}A_0(n/k) = O(1)$ , and (A4) thus follows directly for each  $\varepsilon > 0$ . The second part in point 1. is ensured from (A5) by the continuous mapping theorem. For  $\gamma < -1/2$ , we observe from (A5) that

$$\sqrt{k} \frac{X_{n,n} - x^F}{a_0\left(\frac{n}{k}\right)} \stackrel{d}{=} k^{1/2+\gamma} \frac{(n^{-1}Y_{n,n})^\gamma}{\gamma} + o_p(1).$$

Since we are addressing the case  $\gamma + 1/2 < 0$ , the fact that  $n^{-1}Y_{n,n}$  converges in distribution to a Fréchet random variable suffices to conclude the proof.  $\square$

**Lemma A.3.** *Given the conditions of Theorem 2,*

$$\sqrt{k} \left( \int_{1/2}^1 \frac{X_{n-[2ks],n} - U\left(\frac{n}{2ks}\right)}{a_0\left(\frac{n}{k}\right)} \frac{ds}{s}, \frac{X_{n-k,n} - U\left(\frac{n}{k}\right)}{a_0\left(\frac{n}{k}\right)} \right) \quad (\text{A6})$$

*converges in distribution to a bivariate normal  $(P, Q)$  with zero mean and covariance matrix with entries*

$$\begin{aligned} \text{Var}(P) &= \frac{2}{\gamma} \left( \frac{2^{-(2\gamma+1)} - 1}{2\gamma + 1} - \frac{2^{-(\gamma+1)} - 1}{\gamma + 1} \right), \\ \text{Cov}(P, Q) &= -\frac{1}{\sqrt{2}} \frac{2^{-\gamma} - 1}{\gamma}, \\ \text{Var}(Q) &= 1. \end{aligned}$$

**Proof:** The first component in (A6) shall be tackled by Theorem 2.4.2 of [de Haan and Ferreira, 2006]

with  $k$  replaced by  $2k$  therein. In particular,

$$\begin{aligned} & \sqrt{2k} \int_{1/2}^1 \frac{X_{n-[2ks],n} - U\left(\frac{n}{2ks}\right)}{a_0\left(\frac{n}{k}\right)} \frac{ds}{s} \\ &= \frac{a_0\left(\frac{n}{2k}\right)}{a_0\left(\frac{n}{k}\right)} \sqrt{2k} \int_{1/2}^1 \left\{ \frac{X_{n-[2ks],n} - U\left(\frac{n}{2k}\right)}{a_0\left(\frac{n}{2k}\right)} - \frac{U\left(\frac{n}{2ks}\right) - U\left(\frac{n}{2k}\right)}{a_0\left(\frac{n}{2k}\right)} \right\} \frac{ds}{s} \end{aligned} \quad (\text{A7})$$

Then, under the second order conditions (6) and (7), Theorem 2.4.2 of [de Haan and Ferreira, 2006] yields for the definite integral on the right hand-side of (A7):

$$\begin{aligned} & \sqrt{2k} \int_{1/2}^1 \frac{X_{n-[2ks],n} - U\left(\frac{n}{2ks}\right)}{a_0\left(\frac{n}{k}\right)} \frac{ds}{s} \\ &= \frac{1}{2^\gamma} \int_{1/2}^1 \left\{ s^{-\gamma-1} W_n(s) + o_p(1) s^{-\gamma-1/2-\varepsilon} + o\left(\sqrt{2k} A_0\left(\frac{n}{2k}\right)\right) \right\} \frac{ds}{s} + O_p\left(A_0\left(\frac{n}{k}\right)\right), \end{aligned}$$

where  $\{W_n(s)\}_{n \geq 1}$ ,  $s > 0$ , denotes a sequence of Brownian motions. Under the assumption that  $\sqrt{k} A_0(n/(2k)) = O(1)$ , we obtain as  $n \rightarrow \infty$ ,

$$\sqrt{k} \int_{1/2}^1 \frac{X_{n-[2ks],n} - U\left(\frac{n}{2ks}\right)}{a_0\left(\frac{n}{k}\right)} \frac{ds}{s} = \frac{1}{\sqrt{2}} \int_{1/2}^1 (2s)^{-\gamma} W_n(s) \frac{ds}{s^2} + O_p\left(A_0\left(\frac{n}{k}\right)\right) + o_p(1).$$

We note that the integral above corresponds to the sum of asymptotically multivariate normal random variables. The second component of the random vector (A6) is asymptotically standard normal [cf. Theorem 2.4.1 of [de Haan and Ferreira, 2006]]. Finally, the covariance for the limiting bivariate  $(P, Q)$  is calculated in a straightforward way using similar calculations to the ones in p.163 of [de Haan and Ferreira, 2006].  $\square$

**Proof of Theorem 2:** Let  $h(\gamma) = (\log 2)^{-1} \int_{1/2}^1 \{(2s)^{-\gamma} - 1\}/(-\gamma) ds/s$ , which is defined in (9). Taking the auxiliary function  $a_0$  from the second order condition (6) we write the following normalization of  $\hat{x}^F$  (cf. (A3) and (A7)):

$$\frac{\hat{x}^F - x^F}{a_0\left(\frac{n}{k}\right)} - h(\gamma) = W_n - \frac{1}{\log 2} P_n + Q_n - \frac{1}{\log 2} \int_{1/2}^1 \left( \frac{U\left(\frac{n}{2ks}\right) - U\left(\frac{n}{k}\right)}{a_0\left(\frac{n}{k}\right)} - \frac{(2s)^{-\gamma} - 1}{\gamma} \right) \frac{ds}{s},$$

with

$$\begin{aligned} W_n &:= \frac{X_{n,n} - x^F}{a_0\left(\frac{n}{k}\right)}, \\ P_n &:= \int_{1/2}^1 \frac{X_{n-[2ks],n} - U\left(\frac{n}{2ks}\right)}{a_0\left(\frac{n}{k}\right)} \frac{ds}{s}, \\ Q_n &:= \frac{X_{n-k,n} - U\left(\frac{n}{k}\right)}{a_0\left(\frac{n}{k}\right)}. \end{aligned}$$

Lemma A.3 entails that  $\sqrt{k}(P_n, Q_n)$  is asymptotically bivariate normal distributed as  $(P, Q)$ , i.e. for the remainder proof, we shall bear in mind that  $P_n$  and  $Q_n$  are of order  $k^{-1/2}$ . Proposition A.2 expounds the limiting distribution of  $W_n$  provided suitable normalization, possibly different than  $\sqrt{k}$ . Hence, the crux of the proof is in the following distributional expansion, under the

second order condition (6), for large enough  $n$ :

$$k^{-\gamma} \left( \frac{\hat{x}^F - x^F}{a_0(\frac{n}{k})} - h(\gamma) \right) = k^{-\gamma} W_n + k^{-(\gamma+1/2)} \left\{ \sqrt{k} Q_n - \frac{\sqrt{k}}{\log 2} \left( P_n + A_0\left(\frac{n}{k}\right) \int_{1/2}^1 \Psi_{\gamma,\rho}^* \left( \frac{1}{2s} \right) \frac{ds}{s} \right) \right\}. \quad (\text{A8})$$

We shall consider the cases  $\gamma > -1/2$ ,  $\gamma = -1/2$  and  $\gamma < -1/2$  separately.

**Case  $\gamma > -1/2$ :** Proposition A.2(1) and Lemma A.3 upon (A8) ascertain the result, by virtue that  $W = Z^\gamma/\gamma$  with  $Z$  a standard Fréchet random variable.

**Case  $\gamma = -1/2$ :** The random component  $W_n$  is asymptotically independent of the remainder  $P_n$  and  $Q_n$ . This claim is supported on Lemma 21.19 of [van der Vaart, 1998]. Hence, the combination of Proposition A.2 with Lemma A.3 ascertains the result.

**Case  $\gamma < -1/2$ :** It is now convenient to rephrase (A8) with a suitable normalization in view of Proposition A.2 and the precise statement thus follows:

$$\sqrt{k} \left( \frac{\hat{x}^F - x^F}{a_0(\frac{n}{k})} - h(\gamma) \right) = \sqrt{k} \left\{ Q_n - \frac{P_n}{\log 2} - A_0\left(\frac{n}{k}\right) \frac{1}{\log 2} \int_{1/2}^1 \Psi_{\gamma,\rho}^* \left( \frac{1}{2s} \right) \frac{ds}{s} \right\} + O_p(k^{\gamma+1/2}).$$

□

**Proof of Corollary 4:** The result follows immediately from Theorem 2, given that the random variables  $W$  and  $N$  are independent. □

## B Proportion of non-admissible EVI and right endpoint estimates

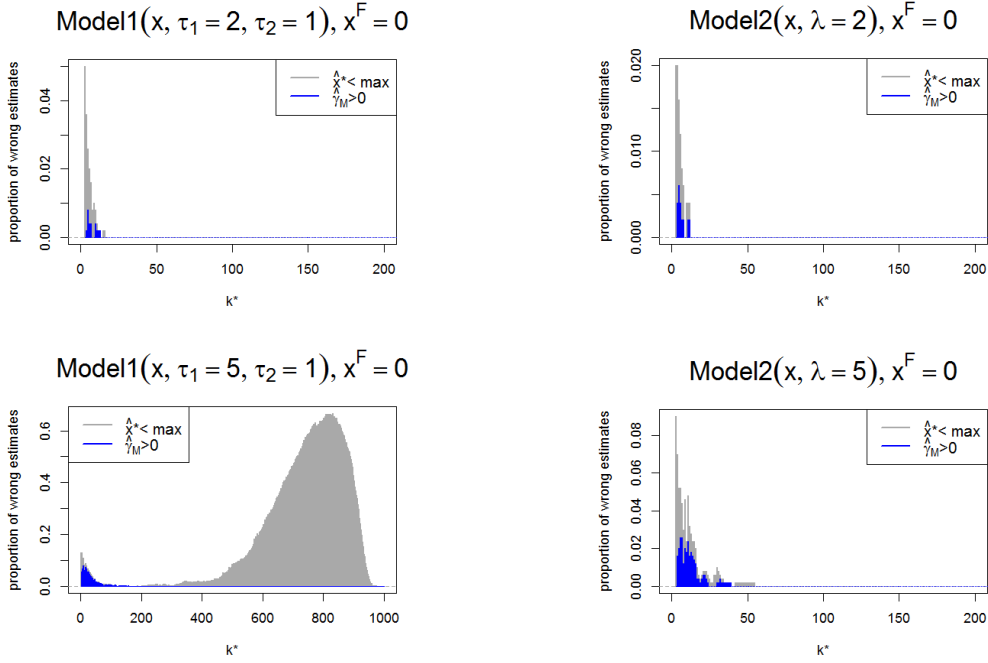


Figure B.1: Model 1 (left) and Model 2 (right): proportions of non-admissible positive estimates, for negative EVI  $\gamma$ , and for the right endpoint, i.e.,  $x^F < x_{n,n}$ , in  $N = 500$  replications of  $n = 1000$  sized samples, plotted against  $k^*$ .

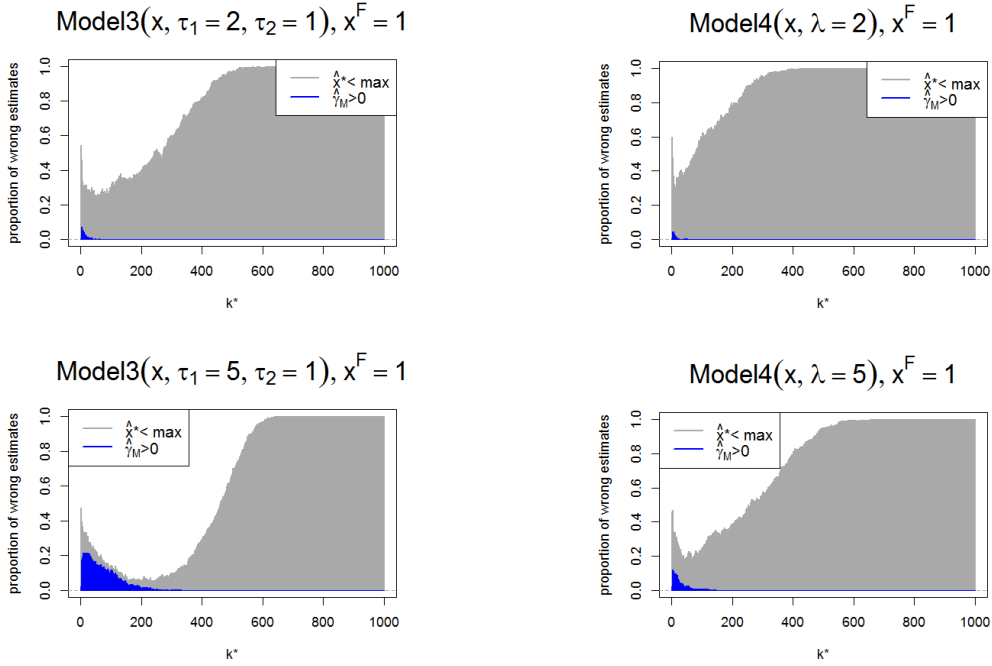


Figure B.2: Model 3 (left) and Model 4 (right): proportions of non-admissible positive estimates, for negative EVI  $\gamma$ , and for the right endpoint, i.e.,  $x^F < x_{n,n}$ , in  $N = 500$  replications of  $n = 1000$  sized samples, plotted against  $k^*$ .

## C Mimicking *lifespan*

In this section we draw similar pictures to the ones of supercentenarians, using a  $n = 1500$  sized simulated sample from Model 3 ( $\tau_1 = 1, \tau_2 = 10$ ) presented in Section 4, shifted with location 110 and scale 20, from which was possible to compare the estimated results from one single sample with the true values, and in particular with the  $x^F = 130$ .

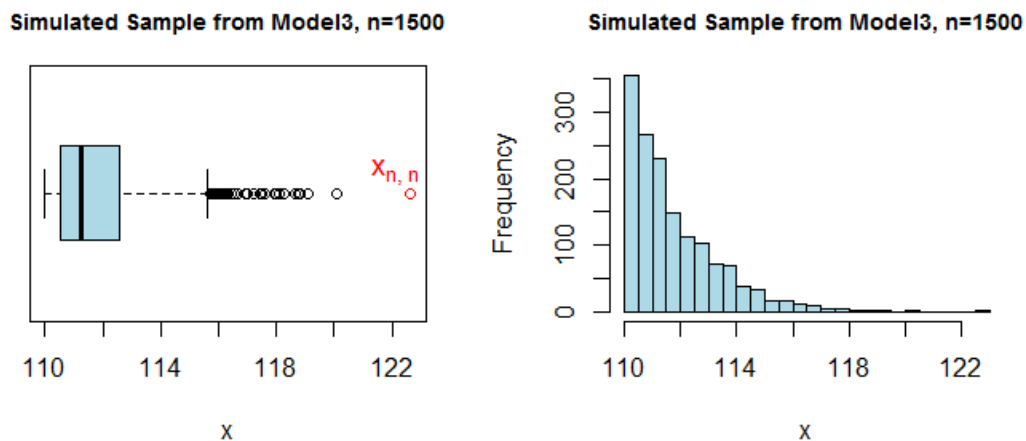


Figure C.1: Boxplot (*left*) and Histogram (*right*): simulated sample of size  $n = 1500$  from shifted Model 3, ( $\tau_1 = 1, \tau_2 = 10$ ), and endpoint  $x^F = 130$ .

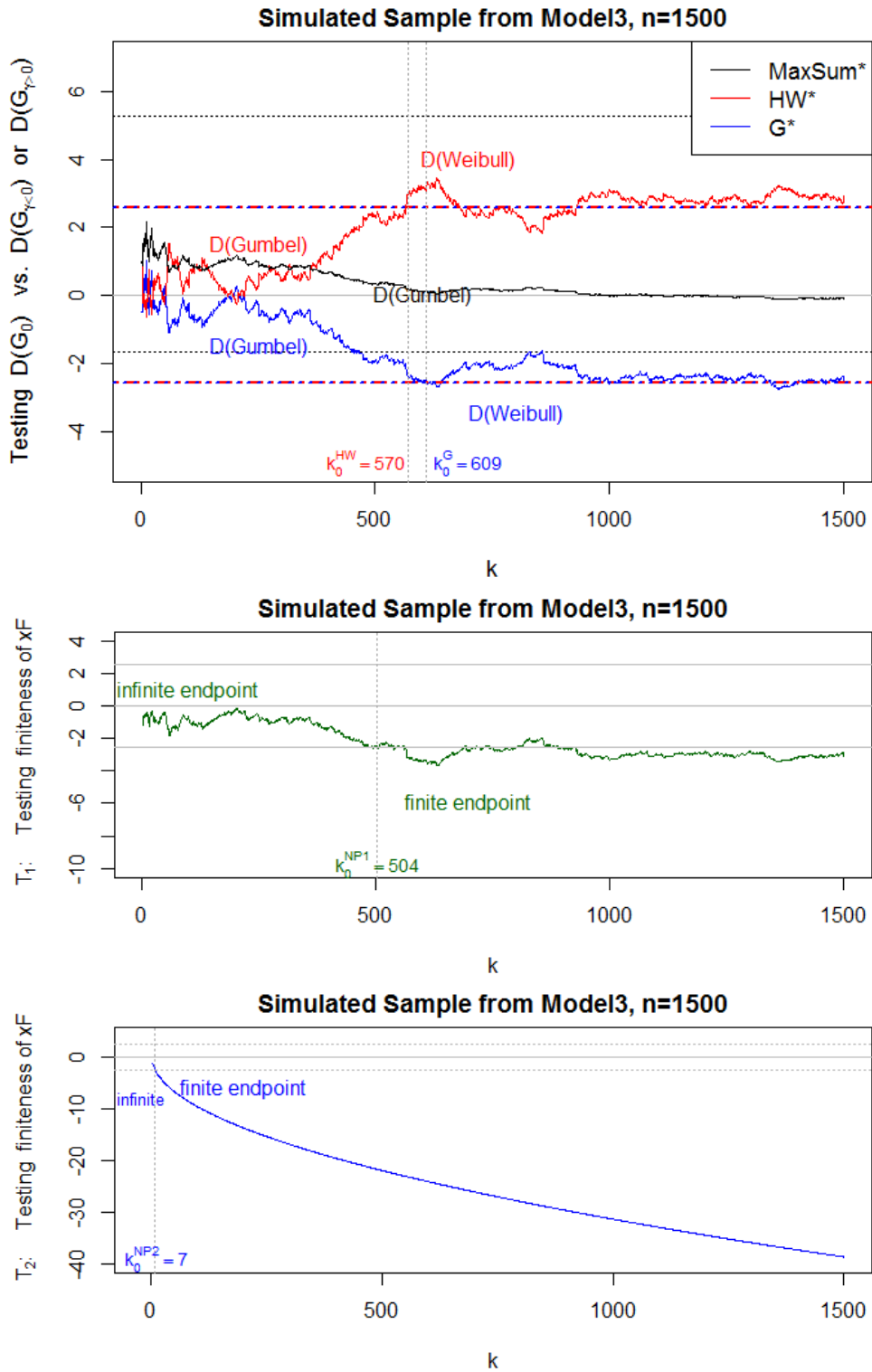
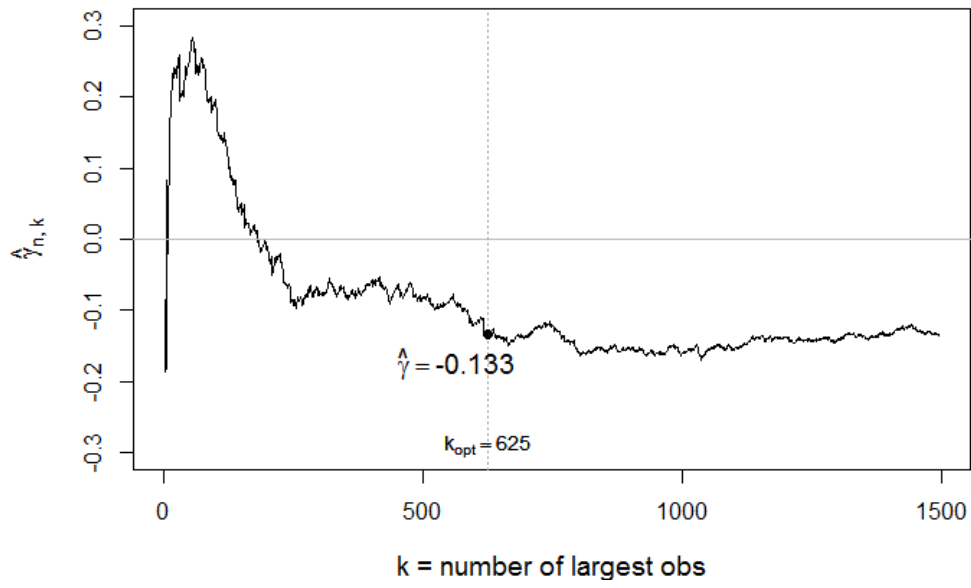


Figure C.2: Testing finiteness of  $x^F$  for a simulated sample of size  $n = 1500$ , from a shifted Model 3 ( $\tau_1 = 1, \tau_2 = 10$ ) and endpoint  $x^F = 130$ .

**Supercentenarians (Women) - Gerontology RG, as of Sept 21, 2014**



**Simulated Sample from Model3, n=1500**

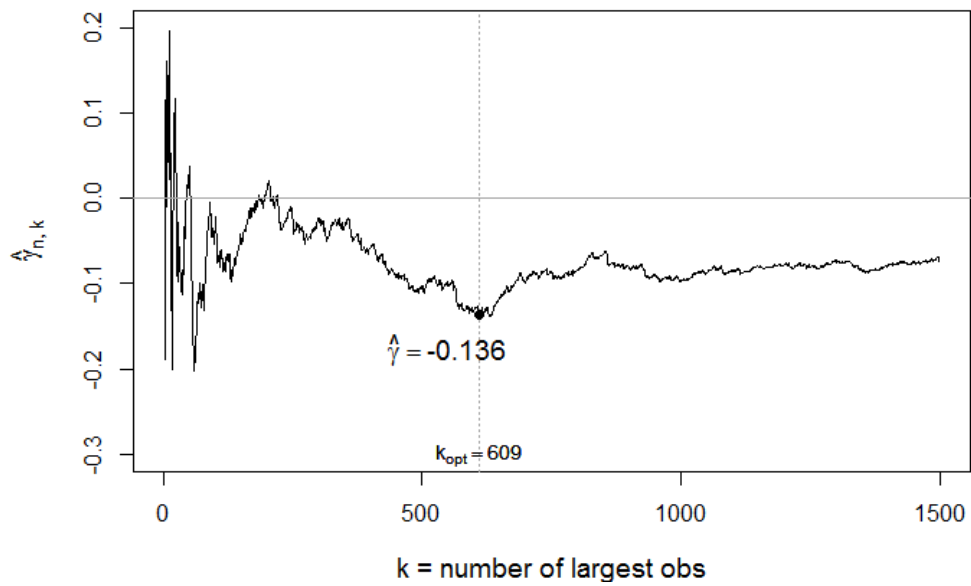


Figure C.3: EVI estimation by  $\gamma_{n,k}^M$ , for verified supercentenarians data set (*up*) and for one simulated sample of size  $n = 1500$  from shifted Model 3, ( $\tau_1 = 1, \tau_2 = 10$ ), and endpoint  $x^F = 130$  (*down*).

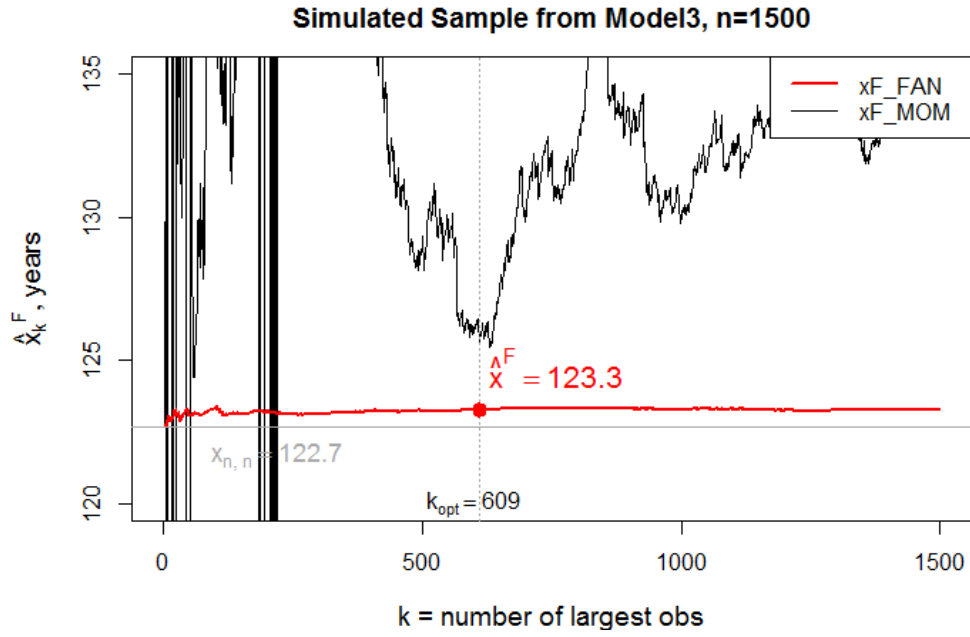


Figure C.4: Endpoint estimation for a simulated sample of size  $n = 1500$  from shifted Model 3, ( $\tau_1 = 1, \tau_2 = 10$ ), and endpoint  $x^F = 130$ .

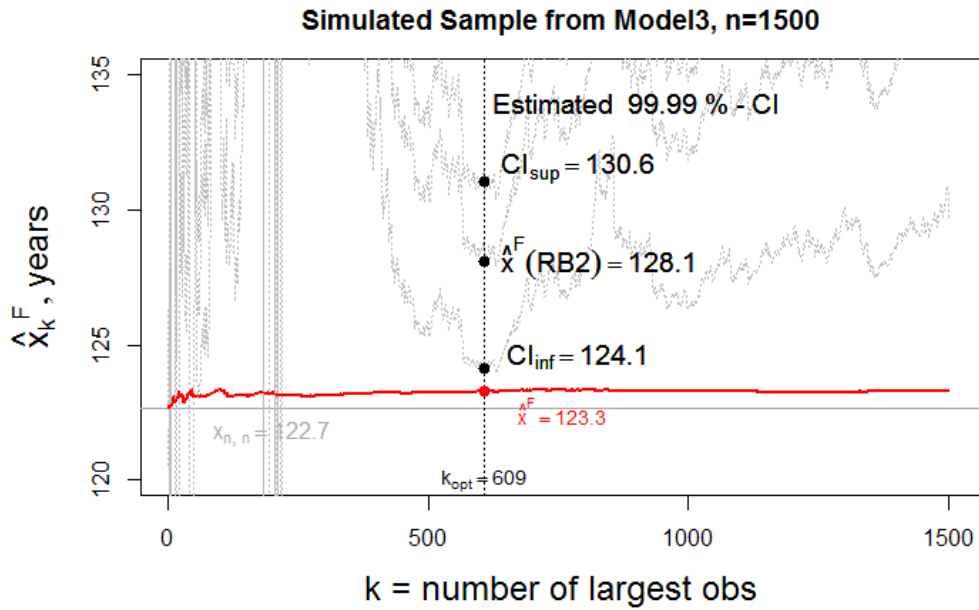


Figure C.5: Endpoint Confidence Bandwidth for  $x^F$  based on a simulated sample of size  $n = 1500$  from shifted Model 3, ( $\tau_1 = 1, \tau_2 = 10$ ), and endpoint  $x^F = 130$ .

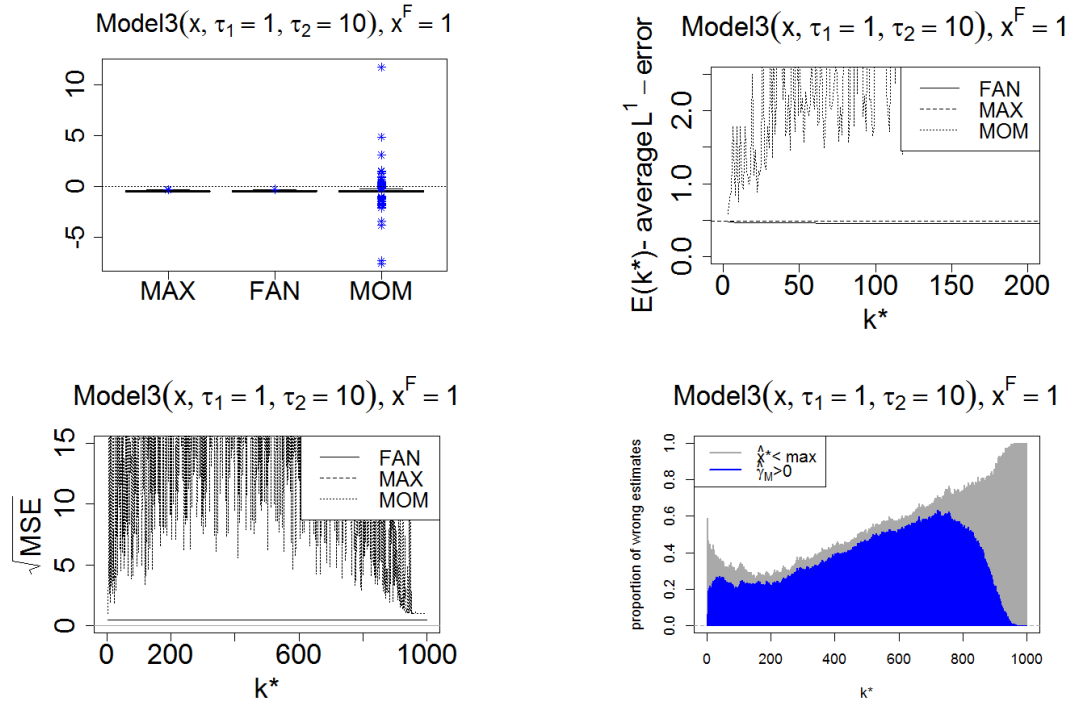


Figure C.6: Model 3,  $x^F = 1$ : Boxplot of  $\varepsilon(j, k_0^*)$ ,  $j = 1, \dots, N$ , for MAX, MOM and FAN estimates;  $E(k^*)$  plotted against  $k^* \leq n/5$ ; root of mean squared error (MSE) and proportions of non-admissible estimates for the EVI  $\gamma(< 0)$  and for the right endpoint  $x^F(\geq x_{n,n})$ , in  $N = 500$  replications of  $n = 1000$  sized samples, plotted against  $k^*$ ,  $k^* \leq n$ .

Table 2: Average  $L^1$ -errors

Model	MAX	FAN	MOM
Model 3 ( $x^F = 1$ ) ( $\tau_1, \tau_2$ ) = (1, 10)	0.482	0.449	0.589

## References

- [Aarssen and de Haan, 1994] Aarssen, K. and de Haan, L. (1994). On the maximal life span of humans. *Mathematical Population Studies*, 4:259–281.
- [Balkema and de Haan, 1974] Balkema, A. A. and de Haan, L. (1974). Residual life time at great age. *Ann. Probab.*, 2:792–804.
- [Bingham et al., 1987] Bingham, N. H., Goldie, C., and Teugels, J. L. (1987). *Regular Variation*. Encyclopedia of Mathematics and its Applications, vol. 27, Cambridge University Press.
- [Cai et al., 2013] Cai, J. J., de Haan, L., and Zhou, C. (2013). Bias correction in extreme value statistics with index around zero. *Extremes*, 16:173–201.

- [Coles, 2011] Coles, S. (2011). Is there an upper limit to human longevity? *AXA Global Forum for Longevity. Conference Proceedings from initial meetings*, pages 96–103.
- [de Haan, 1970] de Haan, L. (1970). *On regular variation and its application to the weak convergence of sample extremes*. Mathematisch Centrum Amsterdam.
- [de Haan and Ferreira, 2006] de Haan, L. and Ferreira, A. (2006). *Extreme Value Theory: An Introduction*. Springer.
- [de Haan et al., 2015] de Haan, L., Klein Tank, A., and Neves, C. (2015). On tail trend detection: modeling relative risk. *Extremes*, 18:141–178.
- [Dekkers et al., 1989] Dekkers, A., Einmahl, J., and de Haan, L. (1989). A moment estimator for the index of an extreme-value distribution. *The Annals of Statistics*, 17:1795–1832.
- [Einmahl and Magnus, 2008] Einmahl, J. H. J. and Magnus, J. R. (2008). Records in athletics through extreme-value theory. *JASA*, 103:1382–1391.
- [Embrechts et al., 1997] Embrechts, P., Klüppelberg, C., and Mikosch, T. (1997). *Modelling Extremal Events*. Springer.
- [Fisher and Tippett, 1928] Fisher, R. A. and Tippett, L. H. C. (1928). Limiting forms of the frequency distribution of the largest and smallest member of a sample. *Math. Proc. Cambridge Philos. Soc.*, 24:180–190.
- [Fraga Alves et al., 2013] Fraga Alves, M. I., de Haan, L., and Neves, C. (2013). How far can Man go? In *Torelli, N., Pesarin, F., and Bar-Hen, A., editors, Advances in Theoretical and Applied Statistics*. Springer, pages 185–195.
- [Fraga Alves and Neves, 2014] Fraga Alves, M. I. and Neves, C. (2014). Estimation of the finite right endpoint in the Gumbel domain. *Statist. Sinica*, 24:1811–1835.
- [Fries, 1980] Fries, J. (1980). Aging, natural death, and the compression of morbidity. *New England Journal of Medicine*, 303:130–135.
- [Girard et al., 2011] Girard, S., Guillou, A., and Stupfler, G. (2011). Estimating an endpoint with high order moments. *Test*, 21:697–729.
- [Girard et al., 2012] Girard, S., Guillou, A., and Stupfler, G. (2012). Estimating an endpoint with high order moments in the weibull domain of attraction. *Statist. Probab. Lett.*, 82:2136–2144.
- [Gnedenko, 1943] Gnedenko, B. V. (1943). Sur la distribution limite du terme maximum d’une série aléatoire. *Ann. of Math.*, 44:423–453.
- [Hall, 1982] Hall, P. (1982). On estimating the endpoint of a distribution. *Ann. Statist.*, 10:556–568.
- [Hanayama, 2013] Hanayama, N. (2013). A discussion of the upper limit of human longevity based on study of data for oldest old survivors and deaths in japan. In *Proceedings 59th ISI World Statistics Congress*, pages 4518–4522.

- [Husler and Peng, 2008] Husler, J. and Peng, L. (2008). Review of testing issues in extremes: in honor of Professor Laurens de Haan. *Extremes*, 11:99–111.
- [Kaufmann and Reiss, 2007] Kaufmann, E. and Reiss, R. (2007). About the longevity of humans. *Section 19.1 of Statistical Analysis of Extreme Values*, pages 453–463.
- [Neves and Fraga Alves, 2007] Neves, C. and Fraga Alves, M. I. (2007). Semi-parametric approach to Hasofer-Wang and Greenwood statistics in extremes. *TEST*, 16:297–313.
- [Neves and Fraga Alves, 2008] Neves, C. and Fraga Alves, M. I. (2008). Testing extreme value conditions – an overview and recent approaches. *REVSTAT - Statistical Journal*, 6:83–100.
- [Neves and Pereira, 2010] Neves, C. and Pereira, A. (2010). Detecting finiteness in the right endpoint of light-tailed distributions. *Statistics and Probability Letters*, 80:437–444.
- [Neves et al., 2006] Neves, C., Picek, J., and Fraga Alves, M. (2006). Contribution of the maximum to the sum of excesses for testing max-domains of attraction. *Journal of Statistical Planning and Inference*, 136:1281–1301.
- [Olshansky et al., 1990a] Olshansky, J., Carnes, B., and Cassel, C. (1990a). In search of methuselah: estimating the upper limits to human longevity. *Science*, 250:634–640.
- [Olshansky et al., 1990b] Olshansky, S., Carnes, B., and Cassel, C. (1990b). In search of methuselah: estimating the upper limits to human longevity. *Science*, 250:634–640.
- [Troen and Cristafalo, 2001] Troen, B. and Cristafalo, V. (2001). *Principles and practice of geriatric surgery*, chapter Cell and molecular aging, pages 8–23. Springer, New York.
- [van der Vaart, 1998] van der Vaart, A. W. (1998). *Asymptotic Statistics*. Cambridge University Press.
- [Vaupel, 2011] Vaupel, S. (2011). Longevity : What is it all about? *AXA Global Forum for Longevity. Conference Proceedings from initial meetings*, pages 2–9.
- [Wang, 1995] Wang, J. (1995). Selection of the  $k$  largest order statistics for the domain of attraction of the Gumbel distribution. *Journal of American Statistical Association*, 90:1055–106.
- [Wilmoth and Robine, 2003] Wilmoth, J. and Robine, J.-M. (2003). The world trend in maximum lifespan. *Population and Development Review*, 29:239–24.